

Genome-wide transcriptome induced in osteoclast-like cells differentiated on three different hard tissues

Inaugural-Dissertation

zur Erlangung des Doktorgrades

der Hohen Medizinischen Fakultät

der Rheinischen Friedrich-Wilhelms-Universität

Bonn

Ghosn Ibrahim

aus Kuwait

2020

Angefertigt mit der Genehmigung
der Medizinischen Fakultät der Universität Bonn

1. Gutachter: Prof. Dr. Andreas Jäger
2. Gutachter: PD Dr. Marjan Nokhbehaim

Tag der Mündlichen Prüfung: 06.03.2020

Aus der Poliklinik für Kieferorthopädie des Zentrums für Zahn-, Mund- und
Kieferheilkunde
Direktor: Prof. Dr. Andreas Jäger

Table of contents

List of abbreviations	6
1. Introduction	10
1.1	Composition and remodeling of hard tissues 10
1.1.1	Bone 11
1.1.2	Dentin 12
1.1.3	Cementum 13
1.2	Osteoclasts 14
1.2.1	Origin 14
1.2.2	Differentiation 14
1.2.3	Activity 15
1.2.4	Coupling of resorption to new bone formation 18
1.2.5	Methods for differentiation of osteoclasts 20
1.3	Difference between humans and mice 22
1.4	RAW 264.7 cells 22
1.4.1	Gene expression profiles of differentiating RAW 264.7 cells 23
1.5	Heterogeneity of osteoclasts 23
1.5.1	Role of the substrate for the heterogeneity of osteoclasts 24
1.5.2	Odontoclasts and cementoclasts 24
1.6	In-vitro-methods for culturing RAW 264.7 cells 25
1.7	Gene expression profiles 26
1.7.1	Methods and technical principles of gene expression analysis 27
1.8	Aims and of the study 30

2. Material and Methods	31
2.1	Morphological changes of the differentiated RAW264.7 cells 31
2.2	Preparation of hard tissue powders 33
2.3	Cell culturing for RNA extraction 37
2.3.1	RNA isolation 37
2.3.2	Quality control of RNA 37
2.3.3	cDNA library preparation 38
2.3.4	Data analysis 39
2.3.5	Ingenuity pathway analysis 41
3. Results	42
3.1	Morphological results 42
3.1.1	Morphological results using dentine discs 42
3.1.2	Results using hard tissue powder 45
3.2	Results of the RNA Sequencing 50
3.2.1	General results of the RNA Sequencing 50
3.2.2	Verification of osteoclast differentiation 53
3.2.3	Impact of different hard tissue substrates 54
3.2.4	Comparison of the different substrates 57
3.2.5	Hierarchical cluster analysis 60
3.2.6	Results of Ingenuity pathway analysis 62
4. Discussion	63
4.1	Discussing the morphological results 63
4.2	Discussing the differentially gene expression levels 64
4.2.1	Differential gene expression level during RAW264.7 cells differentiation 65

5. Summary	76
6. List of Figures	78
7. References	84
8. Acknowledgement	99

List of abbreviations

A	=	Adenine
Acp	=	Acid phosphatases
BGP	=	Bone Gla Protein
BMU	=	Basic multicellular unit
BMMs	=	Bone Marrow Macrophages
bp	=	base pairs
C	=	Cytosine
CD47	=	Cluster of differentiation 47
cDNA	=	complementary Deoxyribonucleic acid
Crtc2	=	CREB Regulated Transcription Coactivator 2
Ctsk	=	Cathepsin K
Cx3cr1	=	C-X3-C Motif Chemokine Receptor 1
Cxcl2	=	C-X-C Motif Chemokine Ligand 2
Ddit4	=	DNA Damage Inducible Transcript 4
DGE	=	Differential Gene Expression
Dmp1	=	Dentin matrix acidic phosphoprotein 1
DNA	=	Deoxyribonucleic acid
DPBS	=	Dulbecco`s Phosphate-Buffered Saline
DPP	=	Dentin phosphoprotein
DSP	=	Dentin Sialoprotein
ECM	=	Extra cellular matrix
EGR1	=	Early Growth Response 1
ELISA	=	Enzyme-Linked Immunosorbent Assay

et al.	=	et alteri (and others)
FBS	=	Fetal Bovine Serum
FC	=	Fold change
FDR	=	False Discovery Rate
Fzd1	=	Frizzled-1
Fzd7	=	Frizzled-7
G	=	Guanine
GADD45G	=	Growth Arrest and DNA Damage Inducible 45 Gamma
GDF15	=	Growth Differentiation Factor 15
Glut1	=	Glucose transporter 1
HEPES	=	Hydroxyethyl Piperazine Ethan Sulfonic acid
HIF-2 α	=	Hypoxia-inducible factor 2 alpha
HMDS	=	Hexamethyldisilazane
Hspa1	=	Heat shock 70 kDa protein 1
Hyal1	=	Hyaluronidase 1
Ibsp	=	Integrin binding sialoprotein
ID1	=	Inhibitor of differentiation 1
IGF1	=	Insulin-like growth factor 1
IL-18	=	Interleukin 18
IL-1b	=	Interleukin-1b
IL-1 β	=	Interleukine 1 Beta
iNOS	=	inducible nitric oxide synthase
IPA	=	Ingenuity Pathway Analysis
IREB2	=	Iron Responsive Element Binding Protein 2
IBSP	=	Integrin Binding Sialoprotein

Mafb1	=	Maf basic leucine zipper transcription factor
M-CSF	=	Macrophage colony-stimulating factor
MMP-9	=	Matrix metalloproteinase-9
mRNA	=	messenger Ribonucleic acid
NA	=	Numerical Aperture
NCPs	=	non-collagenous proteins
Ndrp1	=	N-myc downstream-regulated gene 1
Nfatc1	=	Nuclear Factor of Activated T Cells 1
NGS	=	Next Generation Sequencing
Nlrp3	=	Nucleotide-binding domain and leucine-rich repeat protein 3
Nrros	=	Negative Regulator of Reactive Oxygen Species
OPG	=	Osteoprotegerin
Opn	=	osteopontin
ORF	=	Open Reading Frame
Oscar	=	Osteoclast-associated receptor
PBMCs	=	Peripheral Blood Mononuclear Cells
PBS	=	Phosphate-Buffered Saline
PDL	=	Periodontal ligament
PGE2	=	Prostaglandin E2
RANK	=	Receptor activator of nuclear factor kappa- B
RANKL	=	Receptor activator of nuclear factor kappa-B ligand.
RIN	=	RNA integrity number
RLT	=	RNeasy Lysis Buffer
Rn7sk	=	RNA Component Of 7SK Nuclear Ribonucleoprotein
RNA	=	Ribonucleic acid

RNA-Seq	=	Ribonucleic acid sequencing
RT-PCR	=	Reverse Transcriptase Polymerase Chain Reaction
SEM	=	Scanning Electron Microscope
Src	=	Sarcoma
TCP	=	Tissue culture plastic
TNF	=	Tumor Necrosis Factor
TRAP	=	Tartrate-Resistant Acid Phosphatase
Trib1	=	Tribbles Pseudokinase 1
U	=	Uracil
V-ATPase	=	Vacuolar Adenosine triphosphatase
VEGFR2	=	Vascular endothelial growth factor receptor 2
VNR	=	Vitronectin receptor
Wisp	=	WNT1-inducible-signaling pathway protein 1
α -MEM	=	alpha Modification of Eagle's Medium
α v β 3	=	alpha-Vitronectin beta-3

1. Introduction

Tooth movement is a physiologic process that occurs throughout the development of human dentition and it continues throughout lifetime, although at a slower rate. Orthodontists have used this natural phenomenon by superimposing an external artificial force system to align teeth into esthetic and functional positions. A significant component of orthodontic tooth movement involves bone remodeling and growth alteration by the application of mechanical forces. Teeth and bones, both hard tissues, are thus stressed by orthodontic forces, leading to a comprehensive remodeling of bone, periodontal ligament, periosteum, cementum and sutures. Osteoclasts cells are considered to be a major player in this remodeling process (Thomas et al., 2001; Roberts et al., 2004). Root resorption is one of the adverse effects associated with the orthodontic treatment. Many researchers tried to correlate the severity of root resorption with various factors including treatment mechanics or appliance type, amount of force, duration of treatment, extractions, and previous dental treatments (Gonzales et al., 2000; McNab et al., 2000; Mohandesan et al., 2007; Roberto et al., 2007).

To date, it is still unclear what exact aspects of orthodontic treatment may trigger the resorptive and the repair process of a tooth root. Whether the nature of the tissues that are being resorbed has any effect on the behavior or the activity of the osteoclasts, was the purpose of this study. An insight into the molecular mechanisms of osteoclasts differentiation and activity could possibly lead to preventive or therapeutic strategies for dealing with this unwanted side effect by expanding our understanding of the interaction between the osteoclasts and the different hard tissues of the dental root.

1.1 Composition and remodeling of hard tissues

The term "Hard tissue" is given to all the tissues that are mineralized or have a firm intercellular matrix (Farlex, 2012). Humans hard tissues are bone, tooth enamel, dentine and cementum. Hard tissue remodeling is restructuring the tissue, in a highly coordinated process, to achieve the dynamic equilibrium of this tissue. This process can either be physiological or pathological.

Principally, hard tissue remodeling occurs mainly in bone, because of the synchronized activities of different cells, especially osteoclasts and osteoblasts. Compared with bone the

other hard tissue are quite stable structures. In this work we will try to specify the interaction between the osteoclasts and the different hard tissues -in vitro- as a step to improve our understanding of hard tissues damage and injury mechanics, as well as of the phenomenon of healing and hard tissue remodeling.

1.1.1 Bone

Bone is a mineralized connective tissue that exhibits four types of cells: osteoblasts, bone lining cells, osteocytes, and osteoclasts (Buckwalter et al., 1996). Bone exerts important functions in the body, such as locomotion, support and protection of soft tissues, calcium and phosphate storage, and harboring of bone marrow (Datta et al., 2008).

This hard tissue is composed of inorganic salts and organic matrix (Boskey et al., 2002). The organic matrix contains collagenous proteins (90%), predominantly type I collagen and non-collagenous proteins including osteocalcin, osteonectin, osteopontin, fibronectin and bone sialoprotein II, bone morphogenetic proteins (BMPs), and growth factors (Boskey et al., 2002).

The inorganic material of bone consists of phosphate and calcium ions. Calcium and phosphate ions nucleate to form the hydroxyapatite crystals, which are represented by the chemical formula $\text{Ca}_{10}(\text{PO}_4)_6(\text{OH})_2$, and represent 55% of bone in weight. Together with collagen, the noncollagenous matrix proteins form a scaffold for hydroxyapatite deposition and this association is responsible for the typical stiffness and resistance of bone tissue (Datta et al., 2008).

Bone can be described as a dynamic tissue that undergoes continual adaption during vertebrate life to attain and preserve skeletal size, shape and structural integrity and to regulate mineral homeostasis. Two processes, modeling and remodeling, support the development and maintenance of the skeletal system. Bone modeling is responsible for growth and mechanically induced adaption of bone. Bone remodeling is responsible for removal and repair of damaged bone to maintain integrity of the adult skeleton and mineral homeostasis (Raggatt and Partridge, 2010).

These processes occur due to coordinated actions of osteoclasts, osteoblasts, osteocytes, and bone lining cells which together form the temporary anatomical structure called basic multicellular unit (BMU) (Andersen et al., 2009).

Bone matrix plays an essential role in the bone homeostasis. The bone matrix can release several molecules that interfere with bone cells activity and, consequently, participates in bone remodeling (Green et al., 1995).

1.1.2 Dentin

Dentin is the hard tissue that forms the bulk of the human teeth. In the coronal part of the tooth, dentin is capped by enamel, which is the hardest substance in the human body and contains the highest percentage of minerals (96 % in weight), and in the root it is covered by cementum which is an important structure in attaching the tooth to the bony socket. (Fig.1)

On a weight basis, dentin is more mineralized than bone or cementum, about 65% in weight (Goldberg et al., 2011). The organic matrix in dentin consists majorly of collagen, mainly type I, and the Non-collagenous molecules and extra cellular matrix proteins (ECM) like: osteopontin, osteocalcin and osteonectin.

Odontoblasts are responsible for odontogenesis. In the course of this process, the cells polarize, elongate and start to display two distinct parts: a cell body and a cell process. At the terminal polarization they produce the dentin with cell bodies located outside the predentine/dentin layer at the periphery of the pulp and the cell processes crossing the predentine and extending inside dentin tubules up to the dentin-enamel junction. In contrast with bone, dentin is not vascularized. Tubules are characteristic of dentin; the diameter of the dentine tubules varies between 2 and 4 micrometers. The number of dentine tubules is about 18.000 and 21.000 tubules per mm². The tubules are more numerous in the inner layer than the outer layer of the dentin (Schilke et al., 2000).

Odontoblasts continue to form the so-called primary dentin, until the tooth becomes functional, when contacts between antagonistic cusps are established. Then the formation of secondary dentin starts immediately and continues slowly throughout life.

Dentin resorption is mediated exclusively by so-called Odontoclasts, cells resembling osteoclasts (Steiniger et al., 2010). The resorption can be internal or external, internal resorption starts from the pulp as a result from chronic pulpitis. In contrast to internal resorption, the external resorption originates in the PDL as a result of inflammatory response after a trauma or orthodontic tooth movement. In this form of resorption, the cementum tissue is to be resorbed firstly till the resorption extends in to dentin.

1.1.3 Cementum

Root cementum is a mineralized tissue covering the entire root surface and functions as a tooth-supporting structure in concert with the periodontal fibers and alveolar bone. Cementum is often referred to as a bone-like tissue. However, cementum is avascular, does not undergo dynamic remodeling and increases in thickness throughout life. Cementum is receiving its nutrition from the surrounding vascular periodontal ligament. On these points, cementum is markedly different from bone (Yamamoto et al., 2016).

Cementoblasts are the cells responsible for cementum formation. When these cells become entrapped in the cementum, they are called cementocytes.

Different kinds of cementum are formed: acellular and cellular, and fibers can be intrinsic or extrinsic, resulting in four types of cementum: 1) Acellular extrinsic fiber cementum, which generally covers the cervical root surface 2) Cellular intrinsic fiber cementum. 3) Cellular mixed stratified cementum, which is seen in the interradicular and apical regions of roots. 4) Acellular afibrillar cementum (Bosshardt and Selvig, 1997) (Fig.1)



Fig. 1: longitudinal section of upper central incisor (taken by the author)

Cementum consists of 45% to 50% inorganic matrix, mainly hydroxylapatite, and 50% to 55% organic matrix by weight, what makes it softer than dentin. The organic portion consists predominantly of collagen type I and non-collagenous proteins like bone sialoprotein and osteopontin, which play important roles in the mineralization process and the binding of collagen fibrils and hydroxyapatite (Bosshardt and Nanci, 1998).

The function of cementum is not only limited to tooth support, it plays an important role in adaptation which means reshaping the root surface during tooth movement, by filling resorbed root surfaces, and compensating for crown wear that results from the masticatory stress loaded on the tooth (Schroeder, 1993).

1.2 Osteoclasts

One important feature of bone is the existence of a cell that continuously resorbs the hard tissues. This cell is called the osteoclast and it can degrade mineralized tissue. Osteoclasts are also responsible for the degradation of dentin and cementum during the root resorption process, which is considered to be physiological in the primary dentition and a pathological process in the permanent dentition.

1.2.1 Origin

Osteoclasts were discovered by Rudolph Albert von Kolliker in the year 1873 (Feyen, 1986). They are giant multinucleated cells that usually contains 10-20 nuclei per cell. Osteoclasts are located on the endosteal surface of Haversian canals surface beneath the periosteum. These cells are generally rare in number- only 2-3 per μm^3 - except at sites of increased bone turnover such as the metaphysis of growing bones. Although potential precursors are found in the peripheral blood and spleen as well as within the bone marrow, mature osteoclasts are rarely observed off the bone surface, except in some diseases such as giant cell tumors (Darling et al., 1997).

Osteoclasts are formed by fusion of mononucleated osteoclast progenitors derived from hematopoietic cell lines of the macrophage/monocyte lineage.

The progenitor cells giving rise to osteoclasts, macrophages, and dendritic cells in the immune system are very closely related (Lucht, 1980).

1.2.2 Differentiation

The progenitor cells require stimulation by macrophage colony-stimulating factor (M-CSF), a cytokine expressed by osteoblasts, and by many other cell types. M-CSF is needed for the proliferation and survival of the progenitor cells. Receptor activator of nuclear factor kappa-B ligand (RANKL) is a member of the tumor necrosis factor (TNF) superfamily whose expression is induced in osteoblastic stromal cells. RANKL is also expressed by

other cells such as activated T Lymphocytes and can be induced in fibroblasts from synovial tissues and from periodontal ligament, whereas gingival fibroblasts seem not to express RANKL (Nakashima et al., 2011; Xiong et al., 2011).

RANKL interacts with its cognate receptor RANK, a type 1 transmembrane protein another member of the TNF receptor family. It functions as a homotrimer, on osteoclast precursors and osteoclasts to promote differentiation of osteoclasts precursors and activation of mature osteoclasts to resorb bone. Addition of RANKL along with M-CSF to normal osteoclast progenitors in vitro in the absence of bone marrow stromal cells is sufficient to induce osteoclastogenesis and resorption (Roodman, 2006) (Fig. 2)

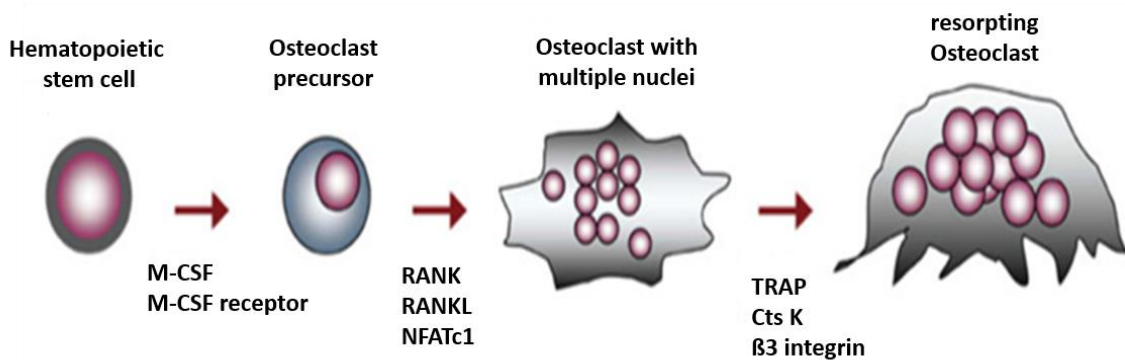


Fig. 2: Formation of multinucleated osteoclasts from Hematopoietic stem cells the figure shows the critical molecules affecting osteoclasts differentiation like RANKL and M-CSF (left). Cell-cells fusion forms multinucleated osteoclasts. Mature osteoclast cell is known by the specific genes like Tartrate-resistant acid phosphatase and Cathepsin K (right). (modified from Lee, 2010)

1.2.3 Activity

Bone must be demineralized before the matrix is accessible for matrix degrading enzymes. The capacity to produce acid in a closed milieu (the resorption lacuna) is what provides the osteoclasts with the unique ability to resorb bone. Therefore, physiological and pathological remodeling and modeling of bone requires osteoclasts.

Polarized osteoclasts have a basolateral domain that doesn't face bone and a resorptive surface that forms a characteristic sealing zone and F-actin ring at sites of bone contact. The integrin $\alpha\beta3$ -also known as vitronectin receptor (VNR)- mediates the attachment of the sealing zone to the bone surface. Inside the sealing zone, the resorptive surface of the

osteoclasts forms a unique and specialized ruffled border at the interface with bone where proteolytic enzymes and hydrogen ions are released to degrade and resorb both the mineral and organic components of the bone matrix.

When osteoclasts are plated on bone surfaces, a characteristic "resorption pit" is formed below the cell within the sealing zone. These resorption lacunae are never seen in the absence of osteoclasts and are not produced by macrophages. The capability to efficiently excavate bone is a unique function of osteoclasts (Holtrop and King, 1977) (Fig. 3 and Fig. 4).

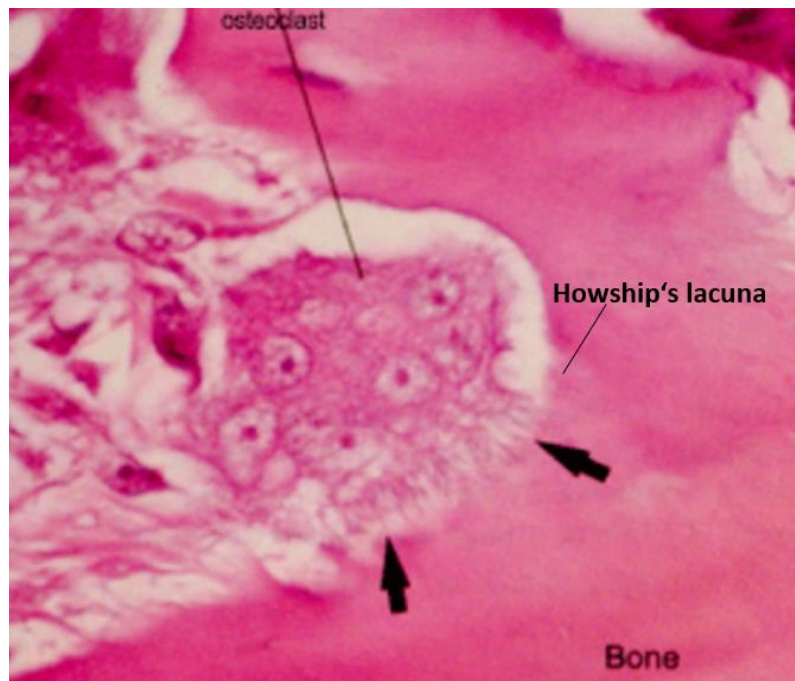


Fig. 3: An osteoclast cell sitting in a Howship's lacuna with the specialized ruffled border (black arrows) that opposes the surface of the bone surface. (modified from Essential Histology 2nd edition, 2001. David H.Cormack)

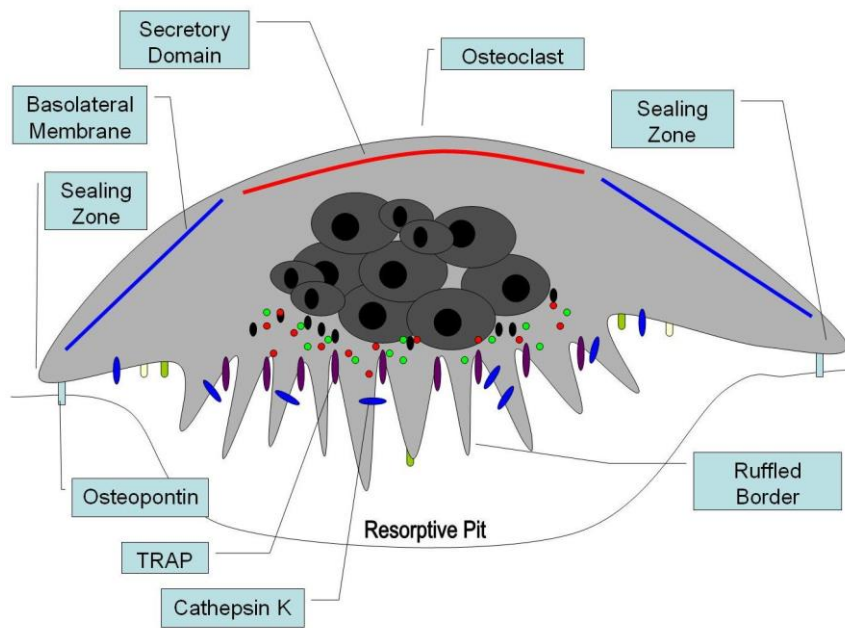


Fig. 4: Illustration of Mature osteoclasts are attached to bone through $\alpha\beta 3$ -expressing vitronectin receptors and in the sealing zone, osteoclasts form the ruffled border in which proton pump subunits and a chloride channel is present. (source: wikidoc.org)

It was unexpectedly found that the receptors for well-known stimulators of bone resorption like parathyroid hormone and 1,25(OH)₂-vitamin D₃ were not present on osteoclasts or their progenitors, but on osteoblasts. Since then it has been found that receptors for most hormones and cytokines stimulating osteoclast formation are expressed by osteoblasts (McSheehy and Chambers, 1986).

More recent work has revealed that osteoclasts vice versa are capable of affecting osteoblastogenesis through secretion of several different signaling molecules (Henriksen et al., 2014). Differentiation of osteoclast progenitors depends on expression of (RANKL) by osteoblasts, which binds to the cognate receptor RANK on osteoclast progenitors. RANK signaling is the most crucial event for the progenitors to differentiate along the osteoclastic lineage. The activation of RANK is depressed by osteoprotegerin (OPG) acting extracellularly by binding to RANKL. Osteoprotegerin is expressed by osteoblasts and stromal cells in bone marrow and most hormones and cytokines stimulating osteoclastogenesis not only increase RANKL but also decrease OPG and, thereby, increase the RANKL/OPG ratio (Nakashima et al., 2012).

These observations demonstrate that osteoblasts are not only bone forming cells, but also cells crucial for regulating osteoclast formation.

1.2.4 Coupling of resorption to new bone formation

One of the most distinctive features of bone remodeling of both cortical and trabecular bone is the precise coupling of bone resorption and formation.

The following sequence is hypothesized as a mechanism for controlling the initiation and coupling of the remodeling process (Roberts and Hartsfield, 2004; Roberts et al., 2006b):

- 1 Inflammatory cytokines (prostaglandins, IL-1 β and others) are released from bone and possibly dentine microdamage.
- 2 Mineralized collagen is exposed to extracellular fluid.
- 3 Osteoblasts react by producing RANKL.
- 4 Pre-osteoclasts from circulating blood have RANK receptors, that are activated by RANKL to form resorbing osteoclasts.
- 5 As bone is resorbed, growth factors are released, which stimulate osteoblasts to produce OPG that will inhibit the activity of the osteoclasts.
- 6 Mononuclear cells move in and coat the resorbed surface with a cementing layer.
- 7 Perivascular osteogenic cells migrate and differentiate to preosteoblasts, which then divide and form osteoblasts (Roberts et al., 1987b).
- 8 Osteoblasts form new bone, fill the resorption cavity and complete the process of remodeling (Fig. 5).

The remodeling process does not change the size or shape of the bones. When the amount of new bone formed is equal to that which is being resorbed, bone remodeling is in balance and bone mass is preserved. Remodeling takes place on surfaces of cancellous and cortical bones, as well as within cortical bone in the Haversian canals. It is more frequent in cancellous bone, which is the reason why metabolic bone diseases like osteoporosis mainly affect bones containing cancellous bone, like the vertebrae and distal radius. It is not known in detail how osteoclasts can recognize damaged bone, but remodeling is believed to be initiated by osteocytes sensing microcracks in the mineralized bone extracellular matrix, resulting in osteocyte apoptosis, which triggers osteoclast formation and resorption of the micro-damaged bone (Martin and Seeman, 2008).

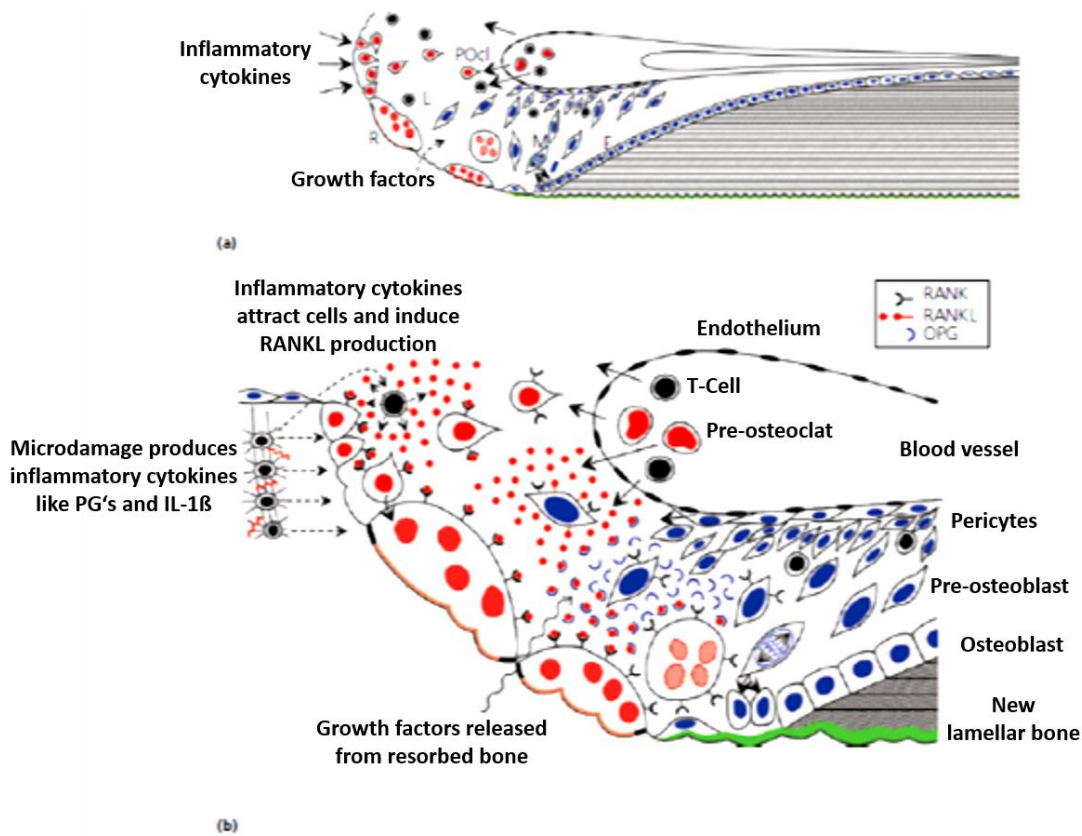


Fig. 5: (a) A longitudinal section through a cortical bone moving to the left via remodeling process demonstrates the intravascular and perivascular mechanisms for coupling bone resorption (R) to formation (F). Inflammatory cytokines will attract Lymphocytes (L) from the circulation, which in turn will recruit pre-osteoclasts (POcl). (b) A magnified view illustrates the proposed mechanism for coupling bone resorption to formation via the genetic RANK/RANKL/OPG mechanism. (left) damaged bone stimulates osteocyte to produce inflammatory cytokines. Osteoblasts react by producing RANKL (red small dots). Differentiated Osteoclasts (bottom left) start resorbing bone which releases growth factors that stimulate the Osteoblasts to release osteoprotegerin (OPG) to stop the differentiation of the osteoclasts. Mononuclear cells (bottom center) build a cementing substance to form a resorption arrest line (shown in green). Preosteoblasts migrate from the circulation and differentiate into Osteoblasts that produce new lamellar bone to fill the resorption cavity (bottom right). (modified from Roberts et al., 2006)

1.2.5 Methods for differentiation of osteoclasts

The ability to culture and study osteoclasts in vitro is one basic technique for studying bone metabolism, the mechanisms of bone disease or any novel skeletal therapeutic agent.

In the past, osteoclasts were isolated as mature cells from neonatal animals (reflecting the requirement for rapid remodeling during growth), by fragmentation of their bones in a suitable liquid medium. The suspended osteoclasts, along with other cell types, including osteoblasts, fibroblasts, and stromal cells, are then allowed to sediment on to bone or dentine slices, on which they excavate typical resorption pits. These methods are now rarely used but knowing them helps in understanding how modern methods were derived (Boyde, 1984; Chambers et al., 1984).

Rodent osteoclast cultures

Mature osteoclasts can be mechanically isolated from long bones of new-born rats (2–4 days). Long bones of new-born rats are isolated, cleared of soft tissues using sterile surgical blades and placed in ice-cold phosphate-buffered saline (PBS). Bone cells are then isolated by finely chopping the bone using a scalpel blade. Osteoclast isolation is performed using medium buffered with HEPES (4-(2-hydroxyethyl)-1-piperazineethansulfonic acid) (Chambers and Magnus, 1982).

Chicken osteoclast cultures

Mature chicken osteoclasts can be isolated from female White Leghorn chicks that have been kept for 7 days on a low-calcium diet, to enhance osteoclastogenesis and bone resorption. After killing, femurs and tibias are collected, cleaned of soft tissue and placed in ice-cold PBS. The bones are then fragmented with sterile surgical blades and sharpened needles used to gently scrape the cells from the bone into fresh PBS (Zambonin et al., 1980).

Rabbit osteoclast cultures

Osteoclasts can be isolated from the long bones of 2–4-day-old rabbits. The limbs are carefully dissected out, the skin removed, and the limbs transferred into a tube containing

ice-cold (PBS). The isolated bones are finely minced into small pieces in a Petri dish with a small volume of culture medium (Coxon et al., 2012).

The development of long-term osteoclast forming cultures, using hematopoietic precursor cells derived from bone marrow, was the key step toward the current methods (Takahashi et al., 1988). For example, mouse osteoclasts can be generated from total bone marrow or by co-culturing previously isolated osteoblasts and bone marrow cells together. Supplementation with factors such as 1,25 Dihydroxy vitamin D3 (1,25(OH)₂D₃) and prostaglandin E2 (PGE₂) is required to promote the expression of RANKL and M-CSF by osteoblasts, leading to osteoclast formation. This method can also be used to generate rabbit and human osteoclast-like cells using whole bone marrow isolated from 2–4 days-old rabbits or human adult volunteer donors respectively (Suda et al., 1992).

The generation and study of osteoclasts was definitely changed by the identification of M-CSF and RANKL as the essential cytokines responsible for the differentiation of hematopoietic stem cells into mature and functional osteoclasts (Takahashi et al., 1999). This method is the most widely used for studying osteoclast function in vitro because of the several important advantages (Yasuda et al., 1998): (1) Large numbers of osteoclasts can be obtained (2) Osteoclastogenesis occurs in cultures that are relatively free of the confounding influence of stromal cells/pre-osteoblasts. (3) The processes of osteoclast formation and activation can be studied independently.

Recombinant M-CSF and RANKL are now widely available, allowing researchers to easily generate osteoclasts in vitro for different study purposes. A variety of cell populations can be driven to differentiate into multinucleated bone resorptive osteoclasts. This includes directly treating adult mouse bone marrow cells or mouse/ human PBMCs with M-CSF and RANKL.

Isolation of human osteoclast precursors

To generate human osteoclasts, peripheral blood mononuclear cells (PBMCs) are first isolated from samples of fresh peripheral/venous blood by density centrifugation. PBMCs are cultured in the presence of M-CSF to expand the precursor population, and then

supplied with both RANKL and M-CSF to generate osteoclasts (Henriksen et al., 2012). Alternatively, the RAW 264.7 murine macrophage cell line can be used as an abundant source of RANKL-sensitive osteoclast precursors (Teitelbaum, 2000) - see 1.4.3 -.

1.3 Difference between humans and mice

Human and mouse share closely related genomes. Both species have similar numbers of protein coding genes, about 30.000. This means that humans share approximately 92% of their genes with mice (Waterston et al., 2002). Morphological and physiological differences between human and mouse do not underlie mainly in the DNA, they derive from changes in non-coding and/or coding sequences in the human and mouse genomes, in other words, the mechanisms that are used by cells to increase or decrease the production of specific gene products like proteins, for example a single gene can code for multiple proteins in a process called alternative or differential splicing. On the other hand, in gene silencing process the expression of a certain gene is reduced (Richard et al., 2003). This turn on (expression) and turn off (repression) mechanism is an important part of development as it determines the function for each cell and allows cells to react to changes in their environments.

1.4 RAW 264.7 cells

Osteoclasts can be generated from some immortalized cell lines, of which the most commonly used is the murine macrophage cell line RAW 264.7 (Collin and Osdoby, 2012). Using a cell line rather than primary cells has several advantages, including wide availability, removing the need to kill a live animal, and ease of transfection.

RAW 264.7 cells are a transformed macrophage cell line isolated from ascites of mice infected with Abelson murine leukemia virus. RAW 264.7 cells can be grown and differentiated on plastic, glass or dentine depending on the experimental purpose and can be analyzed using the same techniques used for primary osteoclasts (Collin and Osdoby, 2012). The number of the differentiated osteoclast-like cells varies considerably with both the number of cells seeded and the passage number of the RAW264.7 cells used. Early and late passages tend to produce low numbers of osteoclasts with optimal results achieved using cells from passages 4 –18 (Marino et al., 2014).

1.4.1 Gene expression profiles of differentiating RAW 264.7 cells

The RAW 264.7 cells are being described as an appropriate model for macrophages. They can perform pinocytosis and phagocytosis. Osteoclasts differentiated from RAW 264.7 acquire activity of Tartrate-Resistant Acid Phosphatase (TRAP) which is the best-known marker for osteoclasts.

A recent study by Taciak et al., investigated phenotype and functional stability of the RAW 264.7 cell line using analyses of their gene expression. They selected the panel of genes involved in macrophage metabolism like: CD11b, CD14, Ireb-2, CD36, iNOS, CD11c, VEGFR2, TRAP and HIF-2 α , which were involved in macrophage functions, and another set of genes, associated with macrophage activation: CD86, HIF-1 α , CD11a, CD18, CD206, CD200R and Glut1 (Taciak et al., 2018). The study concluded that the phenotype and functional characteristics of RAW 264.7 are stable and offer the possibility of long-term growth in culture.

1.5 Heterogeneity of osteoclasts

It's generally assumed that osteoclasts are similar regardless of the skeletal site where they perform their resorption activity, the idea of heterogeneity of osteoclasts was obtained from studies in which osteoclasts activity was influenced by stimulatory or inhibitory agents and from observation in inflammatory bone conditions.

A remarkable observation was made by Kanehisa (1989), who investigated the calcitonin-induced inhibition of osteoclast functionality and found that while most cultured rabbit osteoclasts exposed to calcitonin stopped migrating and started contracting, some cells showed no changes in cytoplasmic motility or general morphology. Another example that points to a heterogeneity of osteoclasts was reported by Owens and Chambers (1993), who found that although M-CSF increased the percentage of migrating rat osteoclasts from 10% to 60%, the remaining 40% of osteoclasts did not respond to this cytokine.

The observations of Hall et al. (1993), showed that while 75% of rat osteoclasts required continued mRNA and protein synthesis to resorb bone when cultured in vitro, some cells still actively resorbed in the presence of the inhibitors actinomycin D and cycloheximide. Furthermore, Nordstrom et al. (1997) observed heterogeneity in the resorption activity of osteoclasts in terms of increased V-ATPase activity in response to a decrease in extracellular pH.

1.5.1 Role of the substrate for the heterogeneity of osteoclasts

The chemical and physical properties of the extracellular matrix (ECM) have a profound influence on the activity and fate of adherent cells. Variations in properties such as matrix molecular composition, and surface topography, can greatly affect many cellular processes, including adhesion, migration, ECM remodeling, cell proliferation, gene expression and cell viability (Geiger et al., 2009; Kunzler et al., 2007). The interaction between the (ECM) of bone and osteoclasts stimulates differentiation, adhesion, migration and polarization (Duong and Rodan, 2001).

Differentiation of monocytes into osteoclasts occurs on unnatural surfaces such as glass, but the formation of sealing zones is generally not observed (Saltel et al., 2004). This implies that different substrates influence the morphology and possibly the function of osteoclasts.

Rumpler et al. (2012) studied the resorption activity of osteoclasts on three different tissues: bone, bleached bone (bone after partial removal of the organic matrix), and dentin. The study revealed lowest resorption activity on bone, significantly higher resorption on bleached bone, and highest resorption on dentin. He interpreted his results with a possible inhibitory impact of the proteins secreted by osteocytes and stored in bone matrix, which are not present in dentin.

1.5.2 Odontoclasts and cementoclasts

Clastic cells are the cells involved in resorption other than monocytes and macrophages which include osteoclasts, odontoclasts, and cementoclasts (Shafer et al., 1963).

Odontoclasts and cementoclasts share the same origin with osteoclasts. Odontoclasts are derived from tartrate-resistant acid phosphatase (TRAP)-positive circulating monocytes and are generally smaller in size, have fewer nuclei and form smaller resorption lacunae than the osteoclasts (Babaji et al., 2017). Cementoclast formation may be induced by Prostaglandin E2 (PGE2) which controls the balance of RANKL/OPG expression levels in cementoblasts. PGE2 stimulates cementoblast-mediated cementoclast activity *in vitro* through the control of RANKL, interleukin-6 (IL-6), and Osteoprotegerin (OPG) synthesized in cementoblasts, mainly through the EP4 pathway. EP4 is the prostaglandin receptor for prostaglandin E2, and mediates the cellular responses to PGE2, in the same matter to the role of PGE2 in osteoblasts (Oka et al., 2007).

Odontoclasts differentiate from circulating progenitor cells which reside in the dental pulp and periodontal ligament (PDL), and they share similar characteristics with osteoclasts such as the expression of cathepsin K, cathepsin D, TRAP, Matrix metalloproteinase-9 (MMP-9), H⁺-ATPase, membrane Type I-MMP expression, and the formation of a clear zone and ruffled border (Wang and McCauley, 2011). The RANK receptor is expressed by odontoclasts and RANKL by odontoblasts as well as by PDL fibroblasts (Harokopakis, 2007). Resorptive cells play an important role in dental health and diseases. The resorbing activity of odontoclasts is controlled by the expression of the OPG/RANKL/RANK system via PDL cells (Oshiro et al., 2001).

During orthodontic tooth movement, on the compressed side of the tooth, RANKL expression is induced, that activates osteoclastogenesis, which facilitates bone resorption (Oshiro et al., 2002). In contrast there is an increase in OPG synthesis on the tensile side of the moving tooth, which in turn inhibits the osteoclastogenesis. The relative expression of OPG and RANKL regulates bone remodelling during orthodontic tooth movement (Tyrovola et al., 2008). Excessive application of orthodontic force induces local tissue degradation and formation of hyalinized areas in the PDL. Macrophages and cementoclasts are involved in the removal of these tissues by a process that includes inflammatory characteristics (Brezniak and Wasserstein, 2002).

Loss of the cementum layer, which protects the underlying dentine, will expose the dentine to osteoclast precursor cells which will differentiate into odontoclasts that attack the dentine tissue and lead to irreversible loss of tooth structure (Olivieri et al., 2012).

1.6 In-vitro-methods for culturing RAW 264.7 cells

Osteoclast differentiation and resorption activity of these cells is regulated by a variety of factors including cytokine signaling (RANKL), integrin-based attachment to substrate (itgb3) and the chemical and physical nature of the mineralized resorption substrate itself (Purdue et al., 2014). The identification of RANKL/RANK signaling as an essential requirement for osteoclast formation, allowed the induction of primary osteoclast precursor cells like bone marrow macrophages (BMMs), splenocytes, and peripheral blood monocytes to osteoclastic differentiation in-vitro by culture in presence of recombinant M-CSF and RANKL (Quinn et al., 1998). The use of these primary cells is associated with

some difficulties like limited availability, variation in response patterns between different preparations and most importantly these primary cells are virtually untransfectable and thus are poorly suited for genetic manipulation and promoter studies (Cuetara et al., 2006). The mouse macrophage cell line RAW264.7 has been identified as a transfectable RANK expressing cell line (Hsu et al., 1999). RANKL has been shown to activate NF- κ B and to induce limited osteoclastic differentiation and bone resorption in RAW264.7 cells (Matsuo et al., 2004). The RAW264.7 cell line is well characterized with regard to macrophage mediated immune, metabolic, and phagocytic functions and is increasingly used and accepted as a cellular model of osteoclast formation and function (Li et al., 1996; Battaglino et al., 2004).

Numerous artificial substrates have been used to study the differentiation and the resorption behavior of osteoclasts, like hydroxyapatite (Narducci and Nicolin, 2009), calcium phosphate (Doi et al., 1999), TCP (Tissue culture plastic) (Detsch et al., 2008). Since fully functional osteoclasts exist especially upon bone surfaces in vivo, different natural mineralized substrates were used to study osteoclasts biology, e.g., bone and dentine (Boyde et al., 1984; Srijarj et al., 2009). These natural substrate favor osteoclasts adhesion and resorption because of the formation of podosomes, which are integrin-based and demonstrate actin-rich adhesive structures (Luxenburg et al., 2007).

Previous studies have demonstrated how bone substrates can regulate osteoclasts gene expression (Rumpler et al., 2013; Purdue et al., 2014).

1.7 Gene expression profiles

Gene expression is the process by which the information is taken from the DNA and converted into a functional product, such as a protein. There are two key steps involved in gene expression: transcription and translation. Transcription is when the DNA is copied to produce an RNA transcript called messenger RNA (mRNA). Translation occurs after the mRNA has carried the transcribed message from the DNA to protein-making factories in the cell, called ribosomes (Crick, 1970).

A cell expresses only a selection of the genes it contains at any one time, which means that the cell can interpret its genetic code in different ways. Controlling which genes are expressed enables the cell to control its size, shape and functions (Papatheodorou et al., 2015).

Gene expression profiling measures which genes are being expressed in a cell at any given moment (Metsis et al., 2004). It is the measurement of mRNA levels, which shows the pattern of genes expressed by a cell at the transcription level (Fielden and Zacharewski, 2001).

1.7.1 Methods and technical principles of gene expression analysis

Different techniques are used to determine gene expression. These include DNA microarray hybridization, which measures the relative activity of previously identified target genes, and sequencing technologies like RNA-Seq that identify all the active genes in a cell in addition to their expression level (Stahlberg et al., 2011).

Hybridization-based approaches involve incubating fluorescently labelled cDNA with custom-made microarrays or commercial high-density oligo microarrays which means that they depend on prior sequence knowledge; therefore, they cannot detect structural variations or isoforms, they produce relative expression levels of genes and suffer from biases.

On the other hand, sequence-based approaches provide a comprehensive view of the transcriptome because they are not dependent on any prior sequence knowledge, instead every single transcript -known or unknown- in the sample is sequenced, which enables the identifications of structural variations such as gene fusion and novel genes. Sequencing data can be reanalyzed when new discoveries are made. RNA-Seq is relatively more expensive than the microarrays but the costs depend on the complexity of the information that is anticipated (Zhao et al., 2014).

RNA-Sequencing can be divided into direct and indirect method. In the direct method, RNA is extracted, isolated and directly sequenced, but this approach is expensive and generally impractical because of the difficulty in RNA handling.

With the indirect method, isolated RNA is converted to a library of cDNA fragments with adaptors attached to one or both ends (Fig. 6). Each molecule, with or without amplification, is then sequenced in a high-throughput manner to obtain short sequences from one end (single-end sequencing) or both ends (pair-end sequencing). The reads are typically 30–400 bp, depending on the DNA-sequencing technology used. Following sequencing, the resulting reads are either aligned to a reference genome or reference transcripts. Alternatively, they are assembled de novo without the genomic sequence to

produce a genome-scale transcription map that consists of both the transcriptional and/or level of expression for each gene (Wang et al., 2009).

Several studies comparing RNA-Seq and hybridization-based arrays have been performed, Marioni et al. (2008) compared the ability of the RNA-Sequencing to identify differentially expressed genes with existing array technologies. They found that RNA-Seq data was highly reproducible, with relatively little technical variation and the differentially expressed genes identified from RNA-Seq overlapped well with those identified by microarray. Fu et al. (2009) designed a study in which they used protein expression measurements to evaluate the accuracy of microarrays and RNA-Seq for mRNA quantification. They showed that RNA-Seq provided better estimates of absolute transcript levels. Zhao et al. (2014) compared both approaches using transcriptome profiling of activated T Cells. They concluded that RNA-Seq is more sensitive in detecting genes with very low expression and more accurate in detecting expression of extremely abundant genes. RNA-Seq also has a wider dynamic range than microarrays.

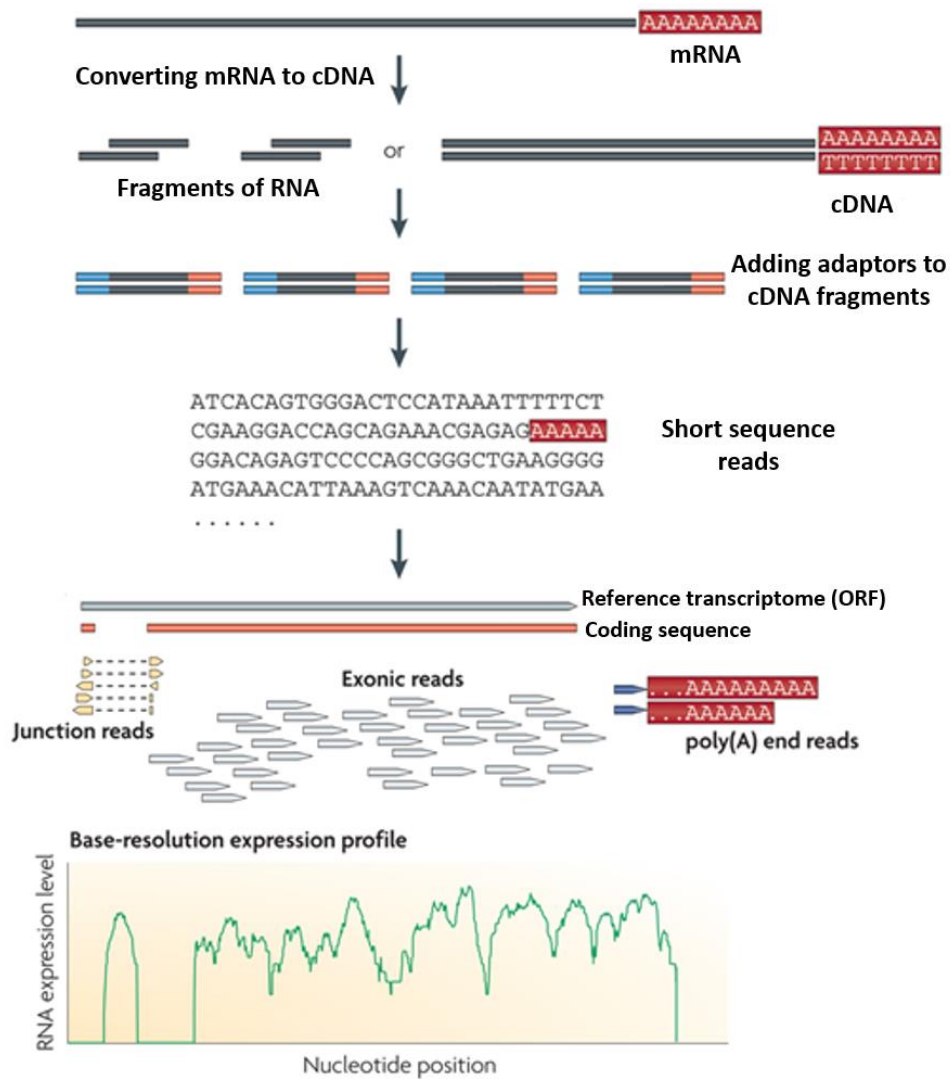


Fig. 6: Illustration of the indirect method of RNA-sequencing. First, long RNAs are converted into cDNA fragments (Top). Sequencing adaptors (blue) are subsequently added to each cDNA fragment and a short sequence is obtained from each cDNA using high-throughput sequencing technology (middle). The coding sequence obtained from the reads is aligned with the reference transcriptome or so-called Open Reading Frame (ORF) to identify the genes. Reads can be divided into: exonic, junction and poly(A) end-reads. These three types are used to generate a base-resolution expression profile for each gene (bottom) (modified from Wang et al., 2009)

1.8 Aim of the study

The aim of this study was firstly to establish a protocol to differentiate the murine macrophage cell line RAW 264.7 into functional osteoclasts on different hard tissue substrates. Thereafter, it was intended to differentiate the cells under different conditions and to examine them with respect to possible morphological differences using light and electron microscope. In a last step, it was planned to identify possible influences of the specific hard tissues on the differentiation process of the RAW 264.7 cells by comparing individual gene expression profiles using RNA sequencing.

It was hypothesized that the macrophagic cells sense the individual hard tissue and while differentiating into mature osteoclasts-like cells respond and develop in a specific way depending on the tissues that they resorb.

2. Materials and methods

2.1 Differentiation of RAW264.7 cells

In order to confirm the ability of RAW 264.7 cells to differentiate into resorbing osteoclasts-like cells, at first, tests were made to identify the morphological changes after differentiation of RAW264.7 cells into osteoclast-like cells. A pre-experiment was made on dentine disc with 0.3 thickness and 4 mm in diameter (Osteosite, Immunodiagnostic Systems Ltd): The murine monocyte macrophage cell line RAW264.7 (obtained from the American Type Culture Collection) was suspended in α -MEM (alpha modification of Eagle's medium) supplemented with 10 % FBS (Fetal Bovine Serum) and antibiotics (100 units/ml of penicillin G sodium and 100 μ g/ml of streptomycin sulfate) at 37°C in an atmosphere of 5% CO₂. 24 dentine slices were used in a 24-wells plate and sample was divided in to four subgroups. In two of these subgroups, 10.000 cells were seeded and in the other two groups 50.000 were seeded. The cells were stimulated for 12 days using 1.9 μ l RANKL and 1.3 μ l M-CSF and the medium was changed every 72 hours.

To determine bone resorption activity of the differentiated osteoclasts-like cells, toluidine blue Staining was performed (Sigma-Aldrich, catalog Number: T3260-5G) (Vesprey and Yang, 2016) in two of the subgroups as described below:

1. Dentine discs were washed with 0.5 ml DPBS /well for one minute.
2. The discs were stained with toluidine blue working solution for 3 minutes.
3. Distilled water was used to wash the dentine discs for five times.
4. After dehydration the discs were examined under light reflected microscope.

In the other subgroups, osteoclasts and morphological surface changes of the dentin slices due to resorption were identified using Scanning Electron Microscope (SEM) according to the following protocol:

1. Fixation with glutaraldehyde (3%, PH 7.3) at room temperature for one hour.
2. Samples were dehydrated in graded ethanol series:
 - 30% EtOH balanced with distilled water for 15 min.

- 50% EtOH balanced with distilled water for 15 min.
 - 70% EtOH balanced with distilled water for 15 min.
 - 80% EtOH balanced with distilled water for 30 min. (two times)
 - 90% EtOH balanced with distilled water for 30 min. (two times)
 - 99.6% EtOH balanced with distilled water for 30 min. (two times)
3. Immersion in HMDS (hexamethyldisilazane) overnight then air dried at room temperature.
 4. Samples were coated with a thin layer of Gold/palladium (AU/Pd) alloy, in a sputtering process as conducting material to prevent charging the samples with the electron beam. (see Fig. 7; 8)
 5. Samples were scanned with high energy beam in a raster scan pattern, which means that the SEM directs a focused electron beam across the samples, which lose energy as it passes through, in form of secondary electrons which are electrons dislodged from the outer surface of the samples. Because of the Everhart-Thorley detectors in the SEM these secondary electrons were registered and magnified three dimensional images were created.



Fig. 7: Dentine discs after Gold/palladium sputtering. (taken by the author)



Fig. 8: Samples loaded in the scanning electron microscope. (taken by the author)

2.2 Preparation of hard tissue powders

To increase the contact surface between the cells and the different hard tissues in vitro, it was decided to prepare a powder from each hard tissue as follows:

Bone powder

A small piece of ilium crest bone, which was remained after a bone grafting surgery, was preserved in 0,5% sodium hypochlorite (NaClO) for 24h to remove remnants of soft tissues and prevent bacterial growth. The powder was produced by cutting the piece of bone using a carbide surgical bur Nr.H161. The estimated size of this powder particles was approximately between 400 – 700 microns.

Dentin and cementum powder

These powders were obtained from extracted human teeth that were preserved in 0,5% NaClO for 24h to remove soft tissues and prevent bacterial growth. Root surfaces were scratched gently with a scalpel to remove the residual PDL tissues (Fig. 9), the apical third of the root was circumferential prepared, because of the increased thickness of cementum

in this third (Yamamoto et al., 2016). Bur Nr.H161 was used in the preparation to produce cementum powder. Presumably, the gained cementum should be primarily cellular cementum due to its location on the dental root (Yamamoto et al., 2016). The estimated size of cementum powder particles was between 600 – 1100 microns (Fig. 10). Dentine powder was produced by preparing the cervical third of the root after removing the superficial layer of cementum with the same bur Nr.H161. The size of dentine particles was estimated to vary between 400 - 1000 microns.

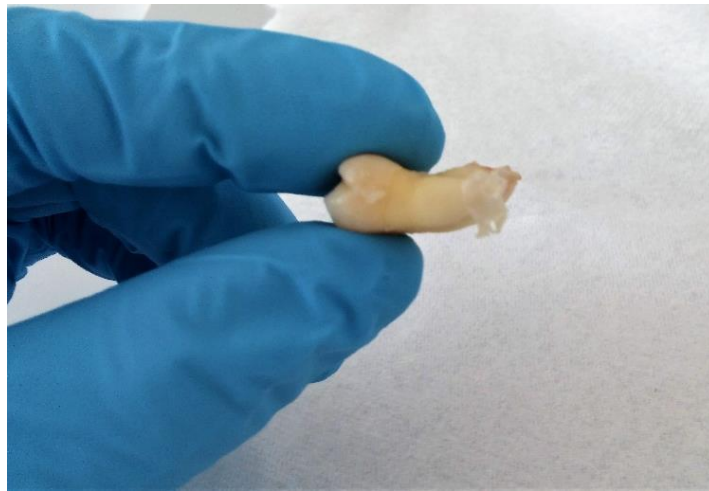


Fig. 9: Preparation of the extracted teeth to obtain the powder. (taken by the author)



Fig. 10: Cementum powder after preparation. (taken by the author)

The morphology of the prepared powder samples from the three hard tissues were visualized using scanning electron microscope and can be seen in figures (11 – 13).

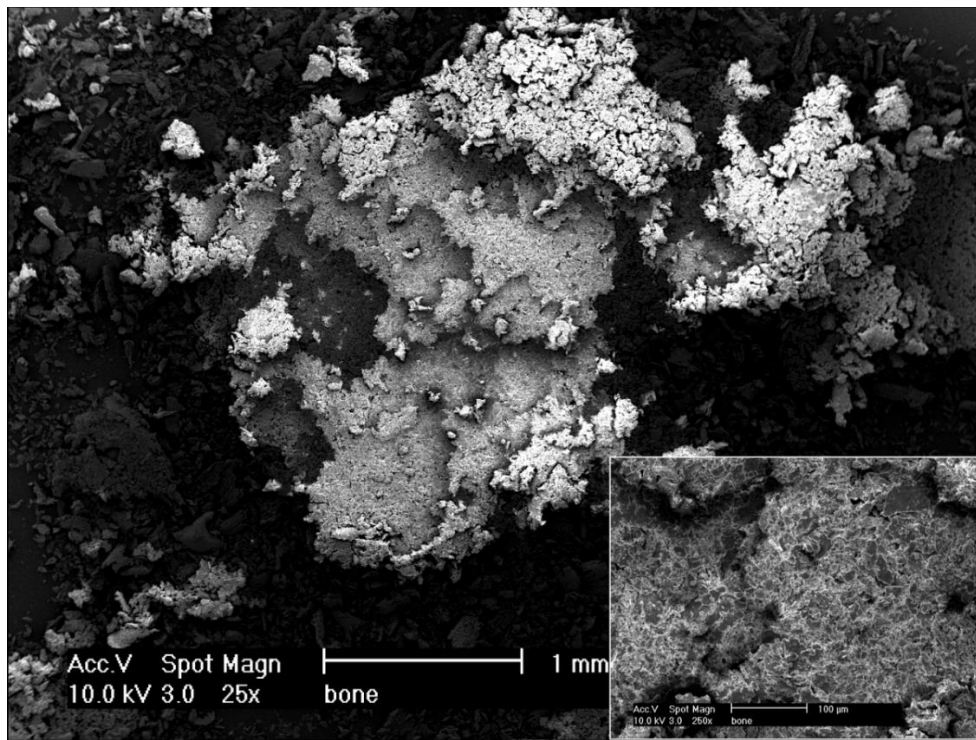


Fig. 11: Bone powder particles under scanning electron microscope in two different magnifications x25 (big picture) and x250 (small picture to the right).

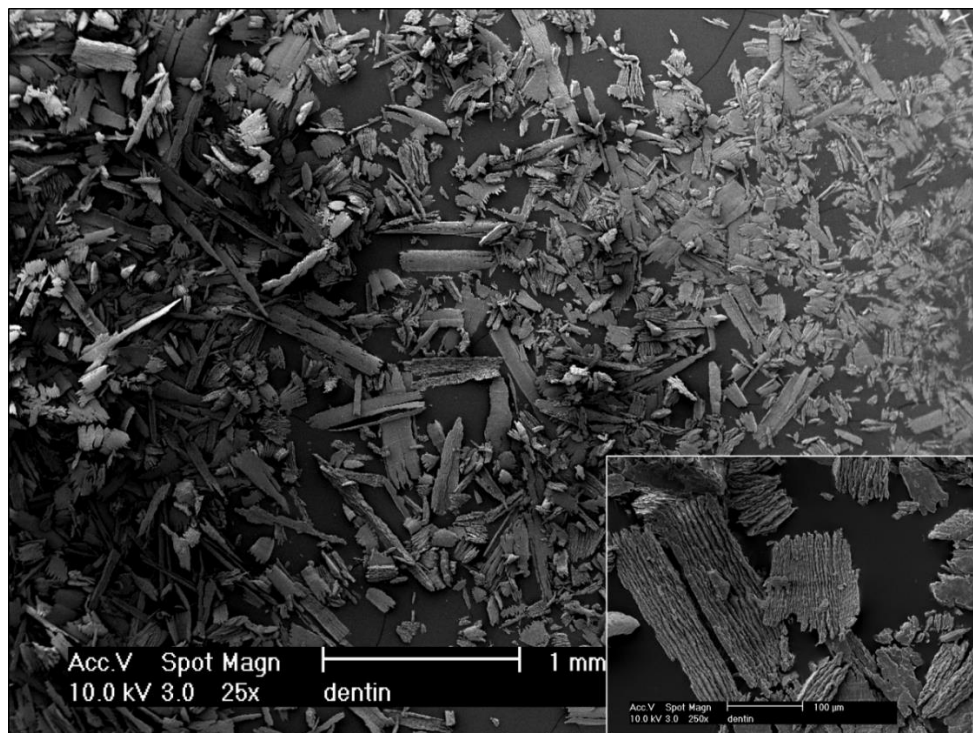


Fig. 12: Dentine powder particles under scanning electron microscope in two different magnifications x25 (big picture) and x250 (small picture to the right).

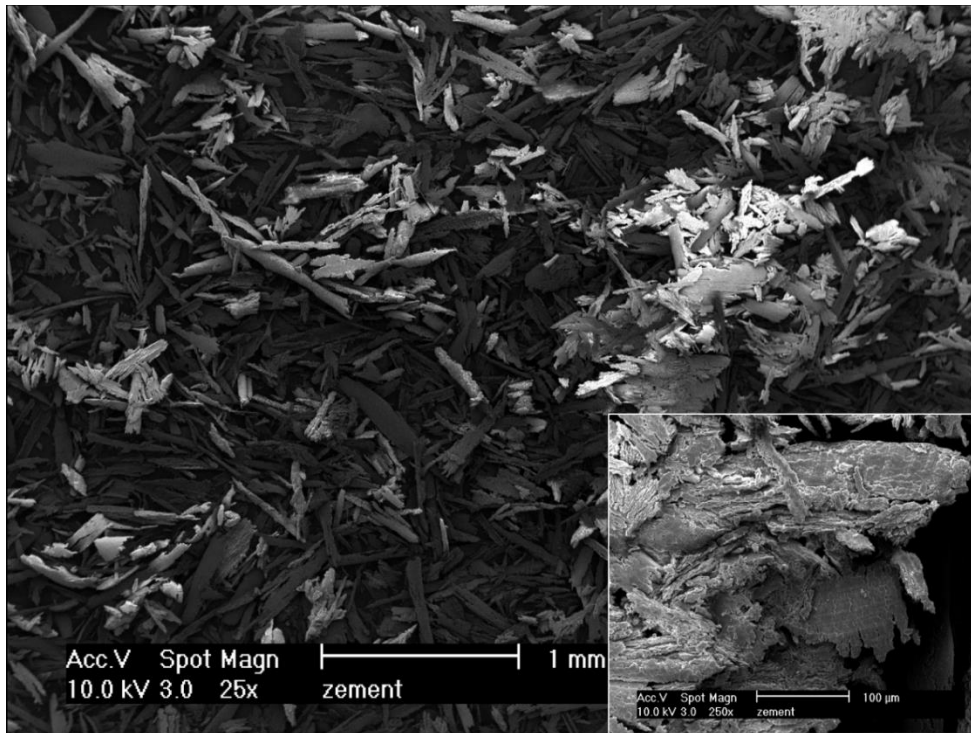


Fig. 13: Cementum powder particles under scanning electron microscope in two different magnifications x25 (big picture) and x250 (small picture to the right).

To determine the osteoclast-like character of the stimulated RAW 264.7 cells, they were cultured on the prepared powders and stimulated with RANKL and M-CSF for 12 days. Four samples were used, one for each hard tissue including bone, dentine and cementum. In another sample, the cells were seeded on glass and served as a control sample. At the end, tartrate-resistant acid phosphatase staining was performed using the Acid Phosphatase (TRAP) Leukocyte Kit (Sigma-Aldrich, Germany) All samples were assessed under light reflected microscope (see Fig. 18- 21). To maintain consistency, the following protocol was used:

1. Washing of the samples with PBS (Phosphate-buffered saline) medium (Two times)
2. Cell fixation with 500 μ l/well 4% paraformaldehyde for 10 Min.
3. Washing with PBS for one minute.
4. Membrane permeabilization with 500 μ l/well 0.05% Triton for 3 Min.
5. Washing with PBS for one minute.
6. TRAP activation with 500 μ l/well Tris-HCL-Puffer at 37°C for 60 Min.

7. TRAP staining with 250 μ l/well solution at 37°C for 60 Min.
8. Washing with water.
9. Counterstaining with 1:2 diluted hemalaun for 5 Sec.
10. Washing with water for 5 minutes.

2.3 Cell culturing for RNA extraction

The murine monocyte macrophage cell line RAW 264.7 was suspended in α -MEM supplemented with 10 % FBS and antibiotics at 37°C in an atmosphere of 5% CO₂ as described before.

The cells were seeded at a density of 3×10^4 cells /well in 6-well plates. Five plates were used, one for each powder sample: dentine, cementum and bone. The powder was utilized in the amount of 0.01 g/well. One of the other two plates served as a positive control sample, with RAW 264.7 cells stimulated with RANKL and M-CSF, and one plate as negative control sample, in which the cells were not stimulated.

The three plates with powder in four wells (0.01 g/well) were sterilized under UV-light for one hour before culturing the cells. Stimulation was done with 10.2 μ l RANKL and 8.6 μ l MCS-F to induce osteoclast-like cells. Medium was changed every 3 days and the total incubation time was 12 days.

2.3.1 RNA Isolation

After stimulation, cells were lysed in RLT buffer (RNeasy Lysis Buffer) and RNA was extracted using the Qiagen RNeasy Mini-Kit (Qiagen, Hilden, Germany) in accordance with the manufacturer's instructions.

2.3.2 Quality control of RNA

RNA concentration and purity were measured using Nanodrop (PeqLab, Erlangen, Germany). This device measures the fluorescent absorbance of nucleic acid samples typically at 260 and 280 nm. In all the samples, RNA concentration was more than 100 ng/ μ L which indicates high cell numbers in the original samples. The A₂₆₀/A₂₈₀ ratio was higher than 2 reflecting purity of the RNA in the samples.

RNA degradation was measured using the Bioanalyzer instrument with the built-in software and the accompanied kit (Agilent Technologies, Santa Clara, CA, USA) which assess RNA integrity by determining the RNA integrity number (RIN). The RIN software algorithm allows for the classification of eukaryotic total RNA, based on a numbering system from 1 to 10, with 1 being the most degraded profile and 10 being the most intact.

2.3.3 cDNA library preparation

The extracted RNAs were converted into a cDNA library representing all the RNA molecules in the samples. This was done using Lexogen QuantSeq 3' mRNA-Seq Library Prep Kit FWD (Vienna, Austria) for genome-wide gene expression analysis by sequencing towards the poly(A) tail. The detailed steps for library preparation using this kit are available at the company's website (www.lexogen.com) the major steps were as follows:

1. mRNA was purified from the total RNA by annealing total RNA to oligo-dT magnetic beads.
2. mRNA strands were broken into multiple small fragments by incubation with fragmentation reagent.
3. Fragmented mRNAs were primed with random primers.
4. cDNAs were synthesized using reverse transcriptase.
5. Second primer was added to synthesize the second strand of the cDNA which resulted in double-stranded cDNA.
6. Double-stranded cDNAs were purified and end-repair was performed.
7. Adaptors are ligated to the end-repaired double-stranded cDNAs.
8. cDNA library was amplified using sequences from the adaptor as primers. Small numbers of cycles (12) were used to amplify the sequences already present.
9. Libraries were normalized and pooled at even volumes, so that each library was equally represented.
10. Normalized libraries were sent to the Next Generation sequencing (NGS) core facility of the medical faculty of the university of Bonn, for cluster generation and sequencing protocol. For more information about this step please refer to www.illumina.com.

2.3.4 Data analysis

The differential expression analysis workflow started with the raw sequence reads, that we received from NGS core facility, and is briefly described as follows:

1. Quality control of reads: the overall quality of the reads was checked by scanning the reads for low confidence bases, biased nucleotide composition or duplicates. This step determines the number of reads which is the basic statistic for the subsequent analyses.
2. Processing of reads: to remove low-quality bases and artifacts such as adapters.
3. Aligning reads to a reference genome: the goal is to find the origin for every read. Each read was mapped to a reference and a sequence alignment was created.
4. Genome guided transcriptome assembly: the alignments are used to determine the genes and transcript models.
5. Calculating expression levels: in this step, the number of reads per gene were calculated and the data were converted to a table of genes together with their read counts.
6. Comparing gene expression levels: statistical analysis was performed using functions implemented in the statistical software R (www.r-project.org), which is an open source software for statistical programming, and Bioconductor as an add-on package. All data were subjected to quantile normalization using the limma package (Ritchie et al., 2015). Briefly, mean values for each sample were calculated from the raw gene expression data. Because of the difference between these mean values, normalization was needed to compensate for this difference by calculating the mean value of the highest expressed gene in each sample. This will be the quantile normalized value for the genes with the highest expression. The same procedure was repeated for the 2nd most expressed gene and the 3rd gene and so on till the least expressed gene in each sample. After quantile normalization, the values for each sample were the same and the original gene orders were preserved. Selection of differentially expressed genes was performed using the following statistical filter criteria: Logarithm Fold change (Log FC) ≥ 0.5 and p-value ≤ 0.05 . Fold change is the ratio of the group mean values. In other words, it describes the quantity change as it shows how many times the expression of a

gene is increased or decreased by dividing the final value by the initial value which will result in a ratio. Therefore, increments will have values bigger than 1 and decrement values will be between 0 and 1. To better visualize the fold changes, the logarithm to the base 2-fold change was used, transcripts with at least 0.5 log fold change were selected.

Adjusting the p-values was essential to exclude false positive values resulting from conducting multiple tests on thousands of expressed genes in a given samples (Jafari and Ansari-Pour, 2019). In this study the p-values were adjusted for multiple testing using Benjamini-Hochberg correction. This method controls the False Discovery Rate (FDR) and calculates the expected proportion of false positives in relation to all positives which rejected the null hypothesis. By FDR, p-values are ranked in an ascending array and multiplied by m/k where k is the position of a p-value in the sorted vector and m is the number of independent tests (Benjamini and Hochberg, 1995). All adjusted p-values were calculated using a Student's t -test.

7. Data visualization: Bar plots were used to visualize the number of differentially expressed genes between the groups of the samples (see Fig. 22; 23). Heatmap and volcano plots were used to visually demonstrate the change of the gene expression level between the samples of the experiment. The volcano plot is used to point out the changes in large data sets composed of replicate data. It summarizes both fold-change and t -test criteria (Cui and Churchill, 2003) In this graphic the negative \log_{10} - adjusted p-values from the gene-specific t test (Y axis) are plotted against the \log_2 fold change between two groups of samples (X axis) and genes with statistically significant differential expression, according to the gene-specific t test, will lie above a horizontal threshold line which represents the nominal significance level. The vertical lines correspond to the up-regulated and down-regulated fold change thresholds. Plotting points in this manner form two areas of interest. The points that are found toward the top of the plot which are too far located either to the left or right side, represent values that display large magnitude fold changes as well as high statistical significance (see Fig. 27 – 33). Finally, Venn diagrams (Oliveros, 2007) were prepared to give an overview about

the numbers of differentially expressed genes between the compared groups (figures 24 – 26). All these plots were created using R software.

2.3.5 Ingenuity pathway analysis

Pathway analysis allows interpretation of the genetic findings by connecting them to known biological processes. The transcriptional data from RNA-Seq were uploaded to Qiagen and evaluated using Ingenuity pathway analysis software (Qiagen IPA 2.4, Systems Inc., Redwood City, CA, USA). This web-based software uses the single nucleotide polymorphism database as genetic variants data. IPA has private curated pathway collections in which each gene is represented in a global molecular network. After uploading the data, the software automatically displays an overview page with information like the number of recognized genes, gene IDs and cellular location. Enrichment analysis was performed to evaluate the data by measuring the percentage of genes that have differential expression in a pathway. In order to get a list of the most relevant pathways, the overlap p-value was used which was calculated using Fisher's Exact test. This value measures whether there is a statistically significant overlap between the reference dataset base genes and the experimentally observed gene expression. Also, the quantity z-score was defined to infer likely activation states of the pathways. The z-score was distributed with zero mean and standard deviation one. The sign of the calculated z-score reflected the overall predicted activation state of the regulator (<0: inhibited, >0: activated). The result page lists several algorithmic generated outputs such as: networks and canonical pathway. For more information please refer to (www.qiagen.com/ingenuity).

In terms of activation, expression and transcription, pathway networks between each comparison groups of the samples were generated. These networks represent the molecular relationship between genes as supported by published data stored in the Ingenuity pathways knowledge base and/or PubMed (Gölz et al., 2016). The canonical pathway visualization is a list of enriched pathways ranked by p-value and percentage of the overlapping gene mapped against the total number of those in that pathway derived from gene expression data (Pita-Jua´rez et al., 2018).

3. Results

3.1 Morphological results

3.1.1 Morphological results using dentine discs

The first experiments were made on dentin discs with two groups of cells with different numbers (50000 and 10000 cells) to determine the appropriate number of RAW 264.7 cells which allows us to identify the differentiated cells easily. Two samples - one of each group- were inspected under light reflection microscope without any staining after different times of incubation (3 and 12 days). Light reflected microscope pictures show the differentiated cells in both groups, resorption at the edge of the dentin discs is also to be seen. After 3 days of incubation, we were able to see the extension of some cells as the initial process of cells fusion in order to form multi nucleated cells. More multinucleated osteoclast-like cells were identified in the 50.000 cells group (see Fig. 14; 15).

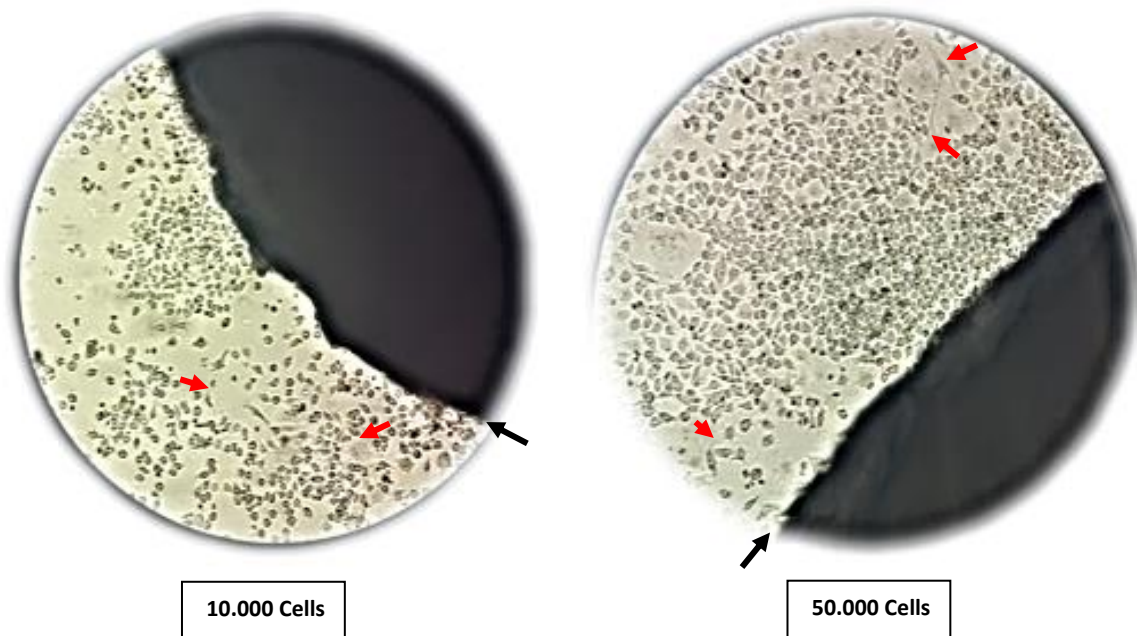


Fig. 14: RAW 264.7 cells under the inverted light microscope (original magnification 10x NA 0.2) after three days of incubation. On the left the sample with 10000 cells and on the right the sample with 50,000 cells can be seen: black areas are the dentine discs the bright areas are RAW264.7 cells. Fusion between the cells is to be identified (red arrows), attached cells are to be seen on the edge of the discs (black arrows).

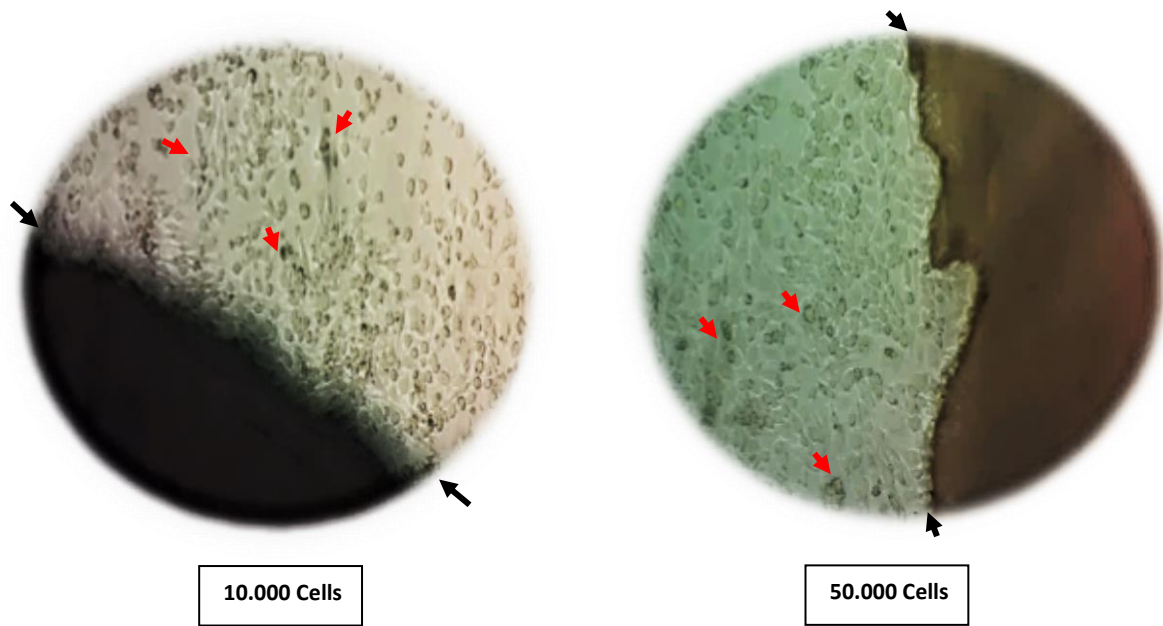


Fig. 15: RAW 264.7 cells under the inverted light microscope (original magnification 10x NA 0.2) at the end of incubation. On the left the sample with 10,000 cells and on the right the sample with 50,000 cells can be seen: black areas are the dentine discs the bright areas are RAW264.7 cells with some cells in fusion to form osteoclast-like multinucleated cells (red arrows), attached cells and the irregular edge of the discs are to be seen (black arrows).

Two other samples -one of each group- were stained with toluidine blue to identify the resorption pits initiated by the osteoclast-like cells after differentiating the RAW264.7 cells with RANKL and M-CSF for 12 days. Dentine discs were examined under light reflected microscope. The resorption pits were clearly notable in the group of 50,000 cells and also more multi nucleated osteoclast-like cells were to be seen in this group (see Fig. 16).

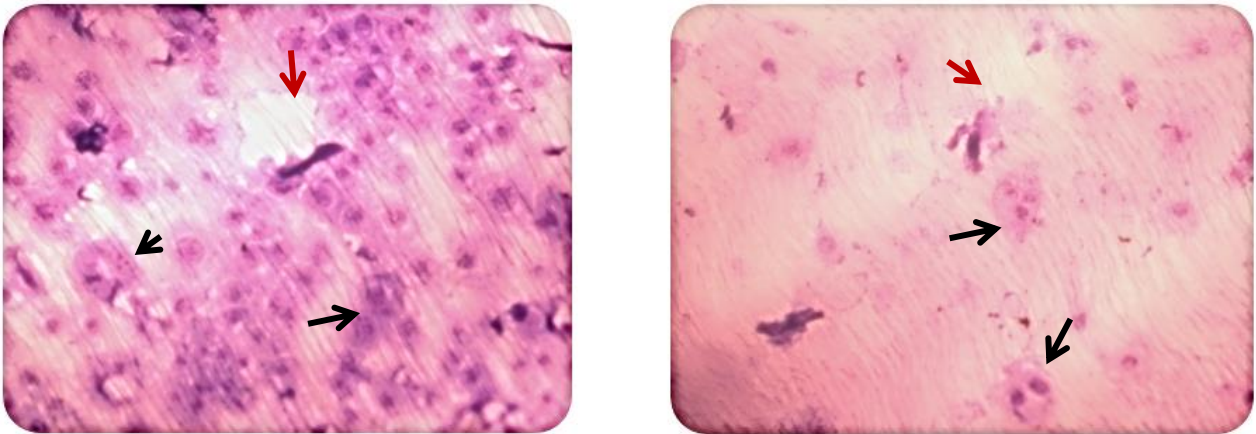


Fig. 16: Differentiated RAW264.7 cells on dentine discs under light inverted microscope in two groups: 50000 cells on the left side 10000 cells on the right. Resorption pits on the dentine discs (red arrows) and multinucleated osteoclast-like cells (black arrows). (original magnification 30x NA 0.2)

The third group was examined under scanning electron microscope, using different magnifications. Fig. 17 shows some osteoclasts and resorption pits on the dentin discs after 12 days of incubation and stimulation with RANKL and M-CSF.

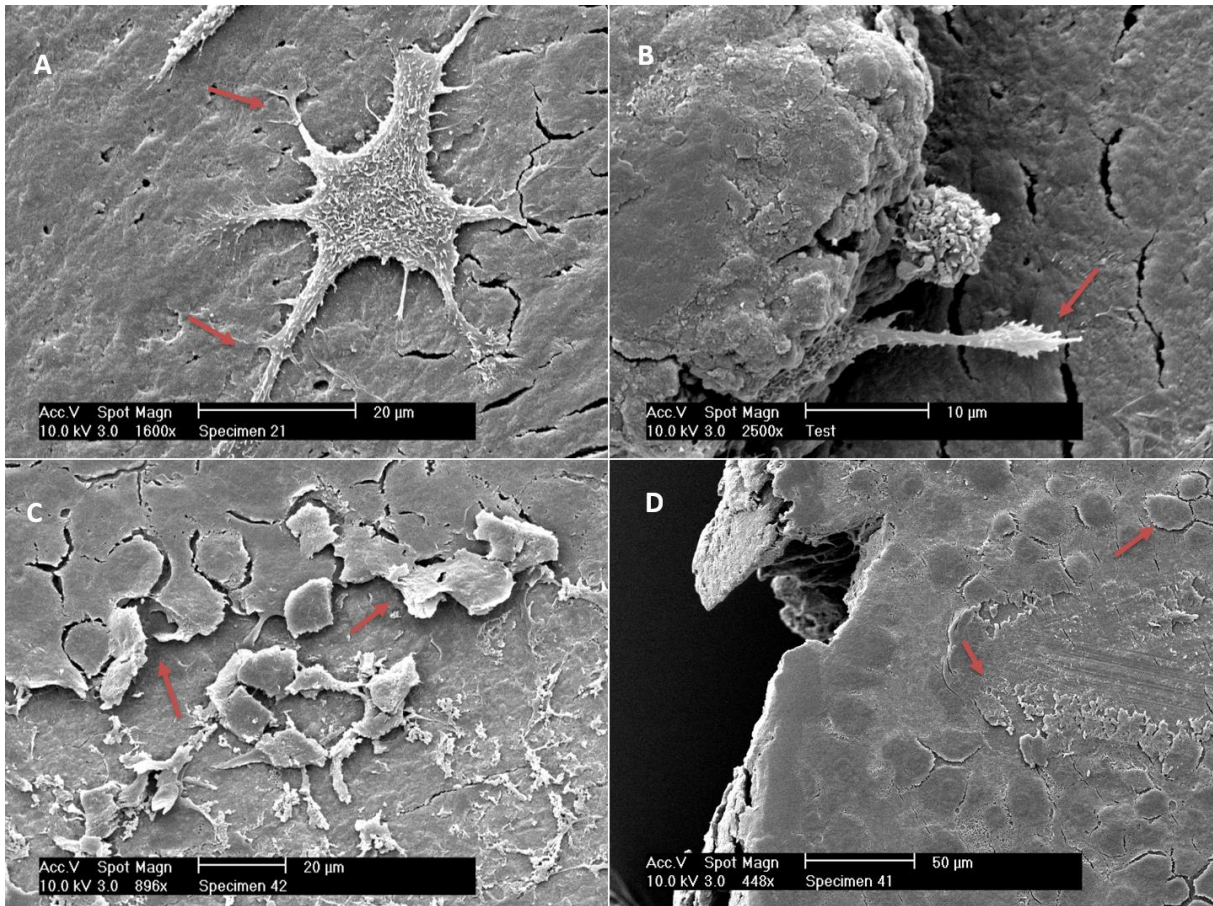


Fig. 17: Dentin discs under scanning electron microscope. High magnification images (A, B Top) show the differentiated osteoclast-like cells with their podosomes (arrows). In low magnification the resorption pits are to be seen (C, D Bottom).

3.1.2 Results using hard tissue powder

TRAP staining was performed on differentiated RAW264.7 cells cultured on three different samples of mineralized hard tissue powder and on glass to determine the osteoclast-character of these cells. TRAP positive cells were to be seen under light reflection microscope in all samples (see Fig. 18; 19; 20; 21).

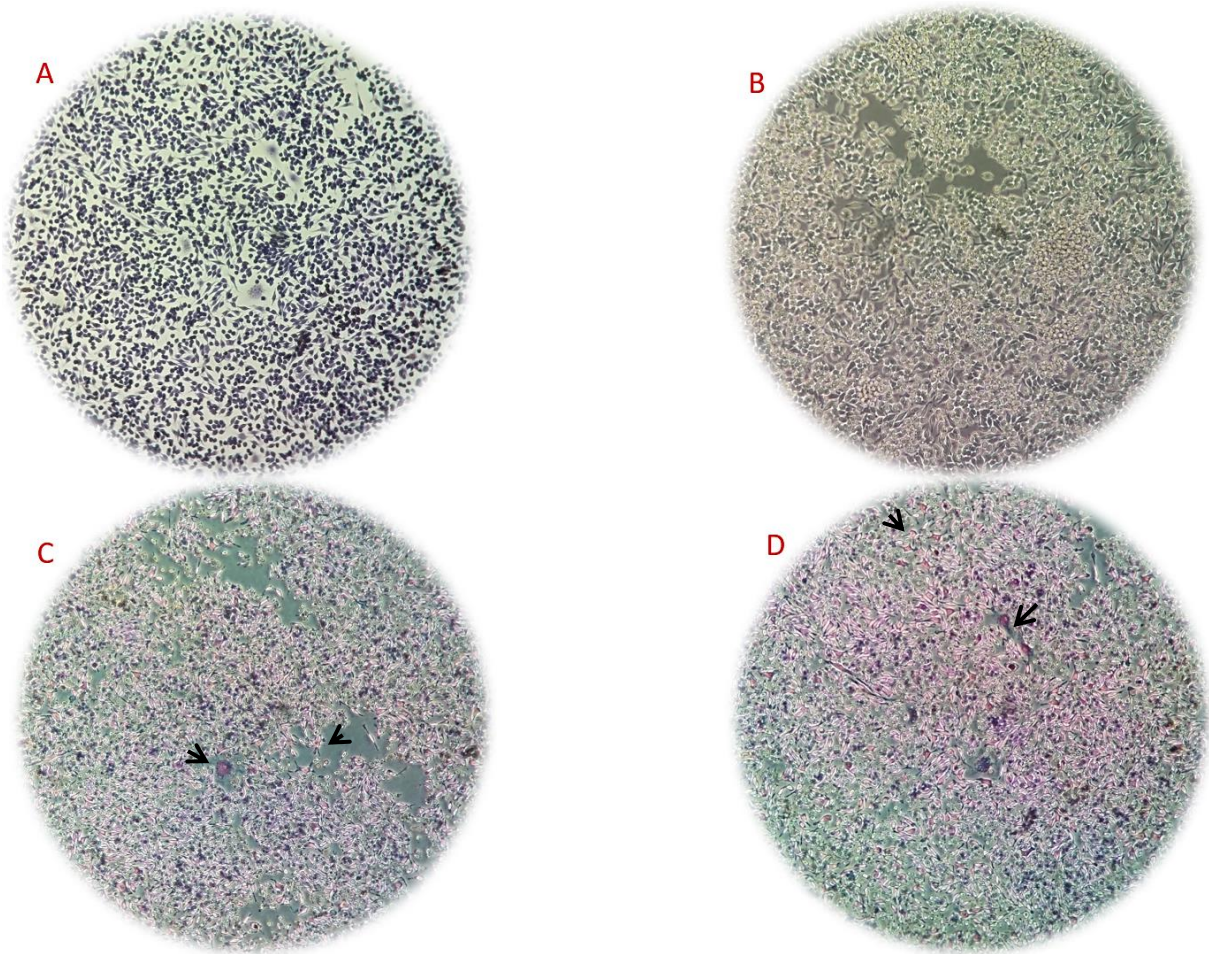


Fig. 18: Control sample of RAW 264.7 cells cultured on glass stimulated for 12 days with RANKL and M-CSF then stained with TRAP. A, B show the cells before staining and C, D show the cells after staining with many differentiated TRAP positive osteoclast-like cells (arrows). (original magnification 10x NA 0.2)

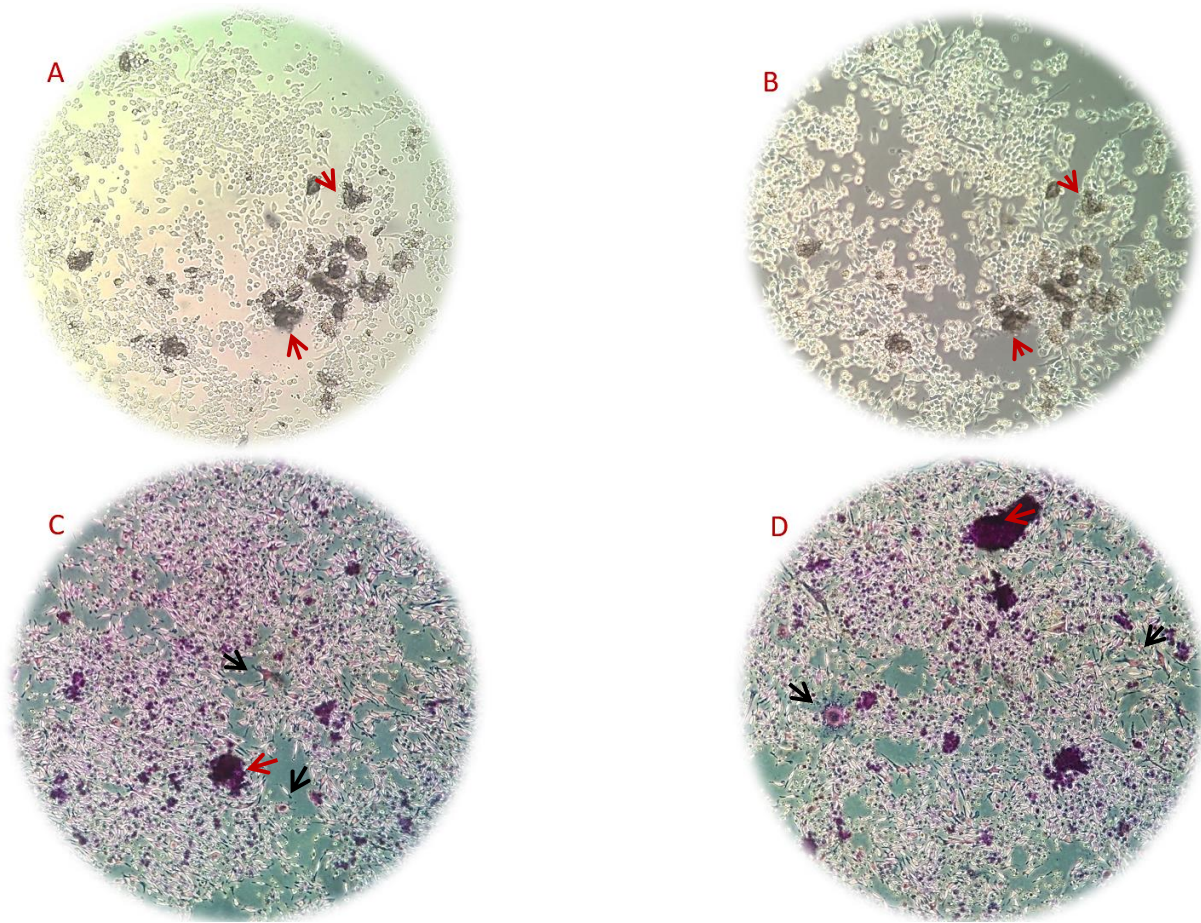


Fig. 19: RAW 264.7 cells cultured with bone powder (red arrows) and stimulated for 12 days with RANKL and M-CSF then stained with TRAP. A, B show the cells before staining and C, D show the Cells after staining with many differentiated TRAP positive osteoclast-like cells (black arrows). (original magnification 10x NA 0.2)

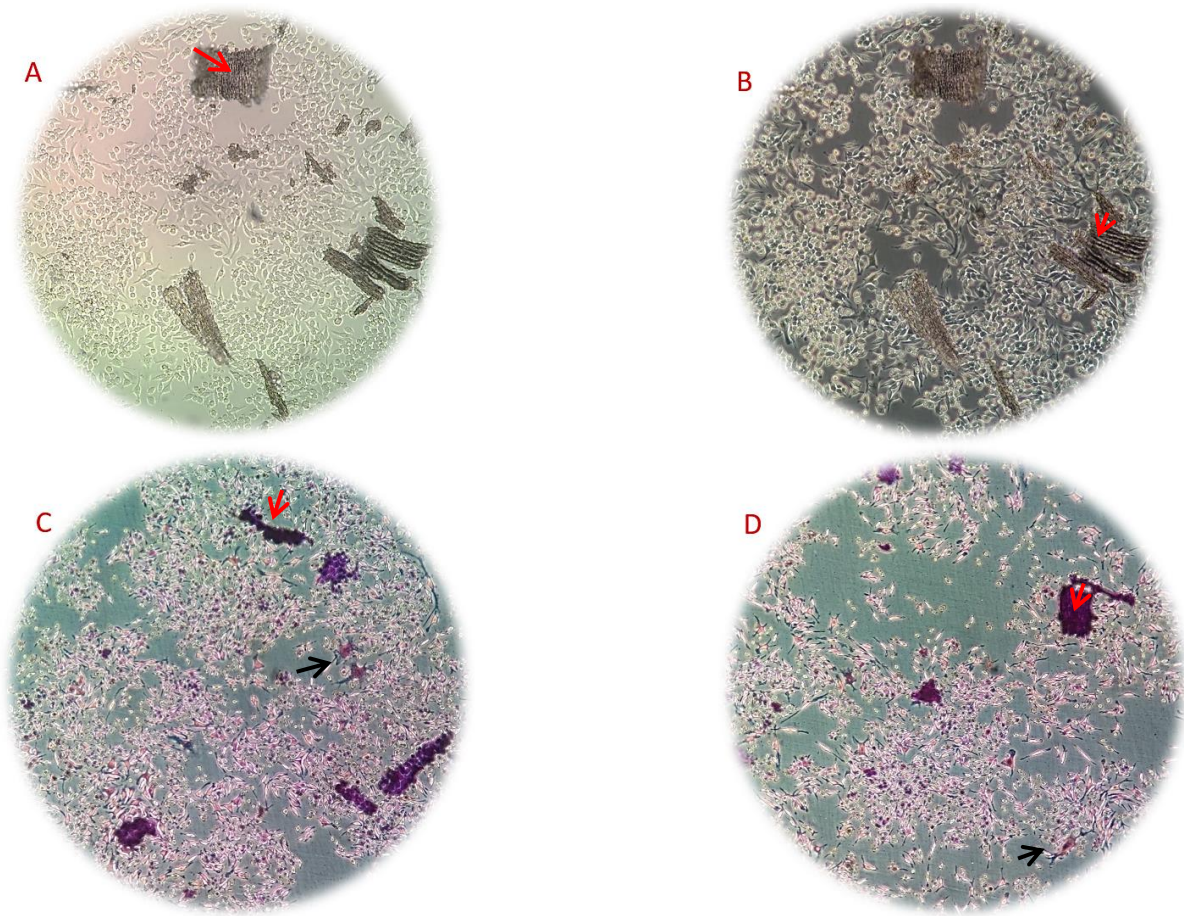


Fig. 20: RAW 264.7 cells cultured with dentine powder (red arrows) and stimulated for 12 days with RANKL and M-CSF then stained with TRAP. A, B show the cells before staining and C, D show the cells after staining with many differentiated TRAP positive osteoclast-like cells (black arrows). (original magnification: 10 x NA 0.2)

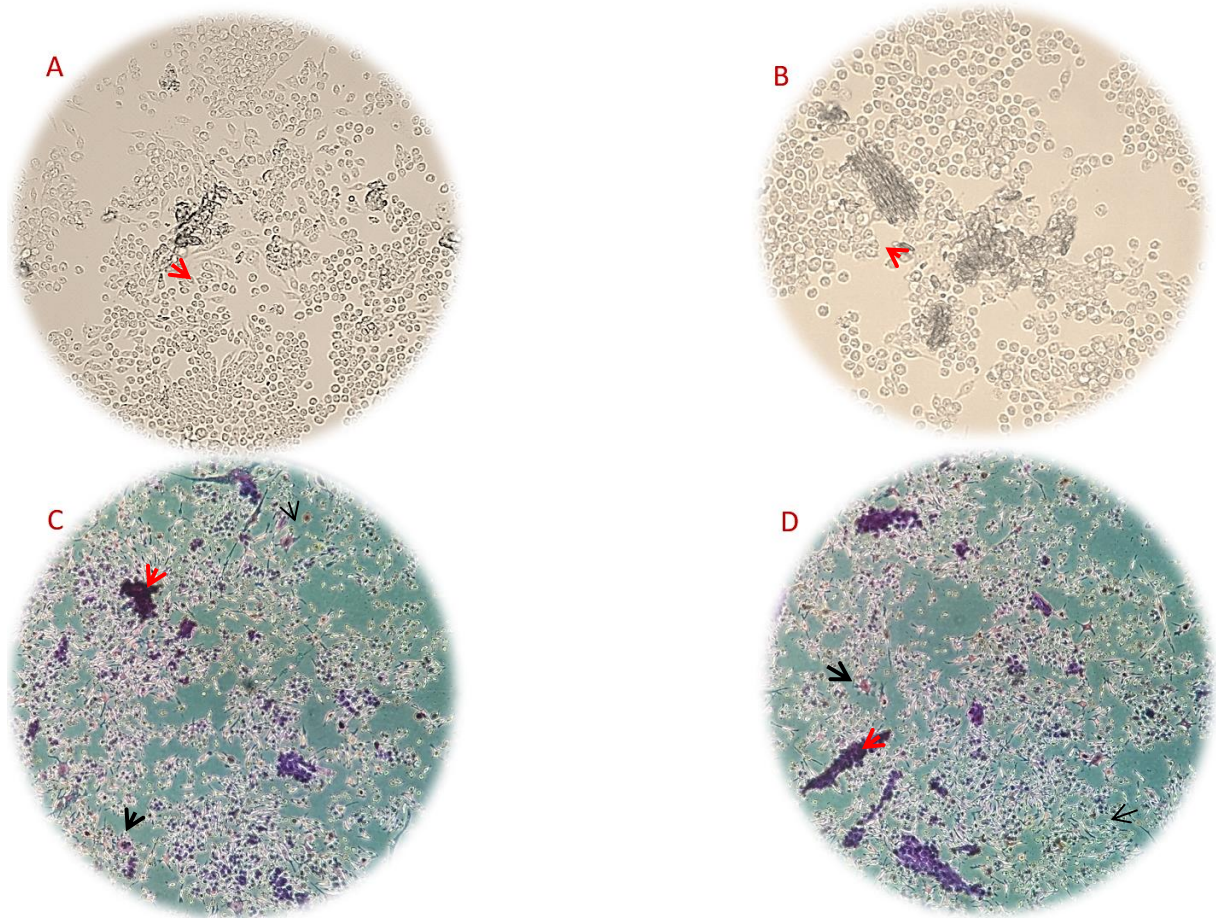


Fig. 21: RAW 264.7 cells cultured with cementum powder (red arrows) and stimulated for 12 days with RANKL and M-CSF then stained with TRAP. A, B show the cells before staining and C, D show the cells after staining with many differentiated TRAP positive osteoclast-like cells (black arrows). (original magnification: 10x NA 0.2)

3.2 Results of the RNA Sequencing

3.2.1 General results of the RNA Sequencing

Initially excluded differential gene expression analysis (DGE) demonstrated a huge number of differentially expressed genes between the groups of the study (Fig. 22).

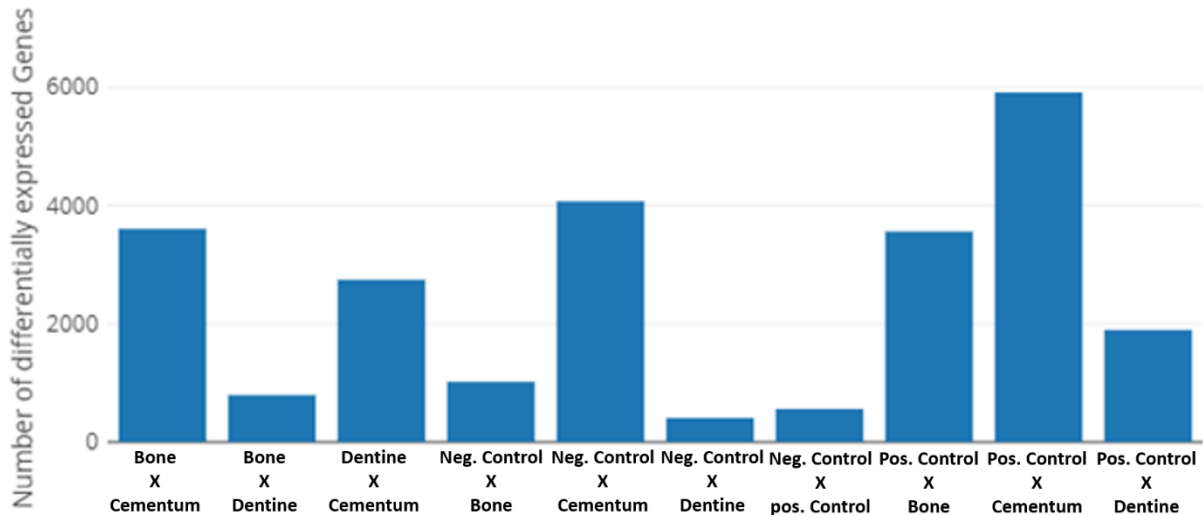


Fig. 22: Bar diagram showing the number of differentially expressed genes between the groups of the samples. (n=4; p <0.05)

To make the results more manageable and getting a better scale we added the logarithm Fold change (logFC) to the analysis (Fig. 23).

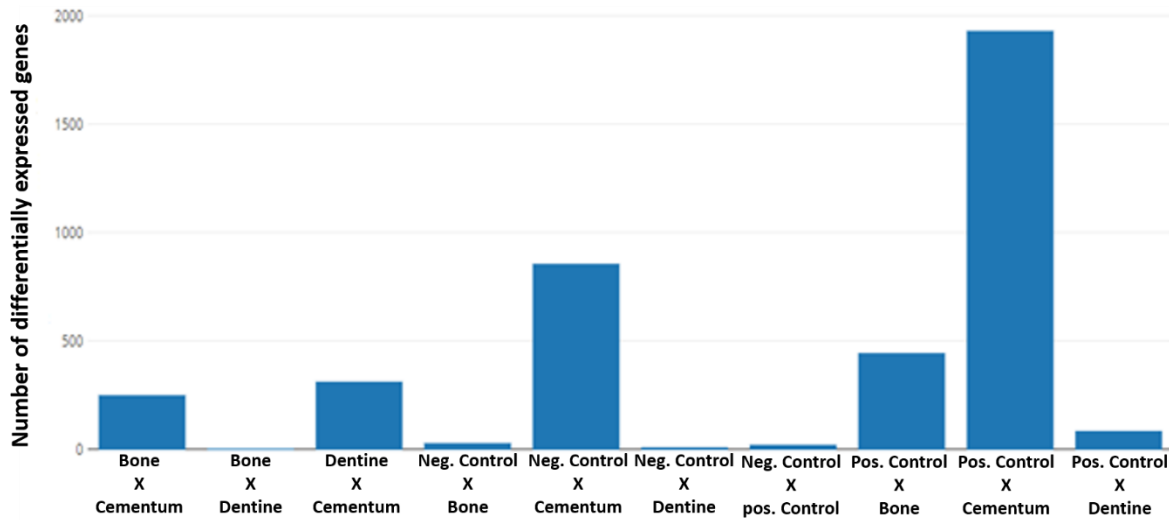


Fig. 23: Bar diagram shows the number of differentially expressed genes between the groups of the samples after using the logarithm Fold change. ($n=4$; $\text{Log FC} \geq 0.5$; $p < 0.05$)

The groups that include hard tissues samples seemingly induced the highest numbers of differentially regulated genes. 1930 transcripts were significantly differentially regulated on cementum compared with the stimulated control group (positive control), 446 between bone tissue and positive control, 87 between dentin and positive control, 857 between cementum and unstimulated control group (negative control), 31 between bone and negative control, 11 between dentine and negative control, 23 between negative and positive control, 314 between cementum and dentine, 252 between bone and cementum and interestingly just one significantly differentially regulated gene between dentine and bone.

The multiple comparisons of the groups are demonstrated with a Venn Diagram (Oliveros, 2007) to illustrate the differences and the similarities between the different groups (see Fig. 24; 25; 26).

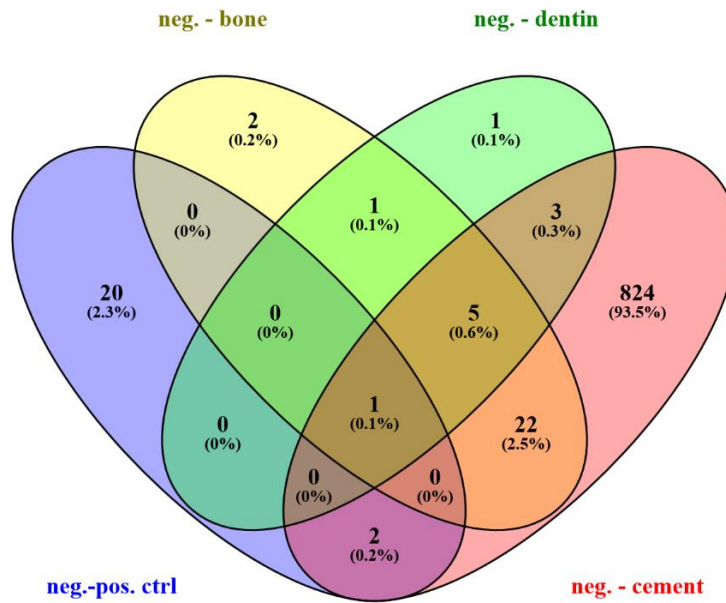


Fig. 24: Venn diagram of differentially expressed transcripts ($\log_{FC} \geq 0.5$; $P < 0.05$), demonstrating differences and similarities in the number of expressed genes between the negative control group and the other groups of the experiment.

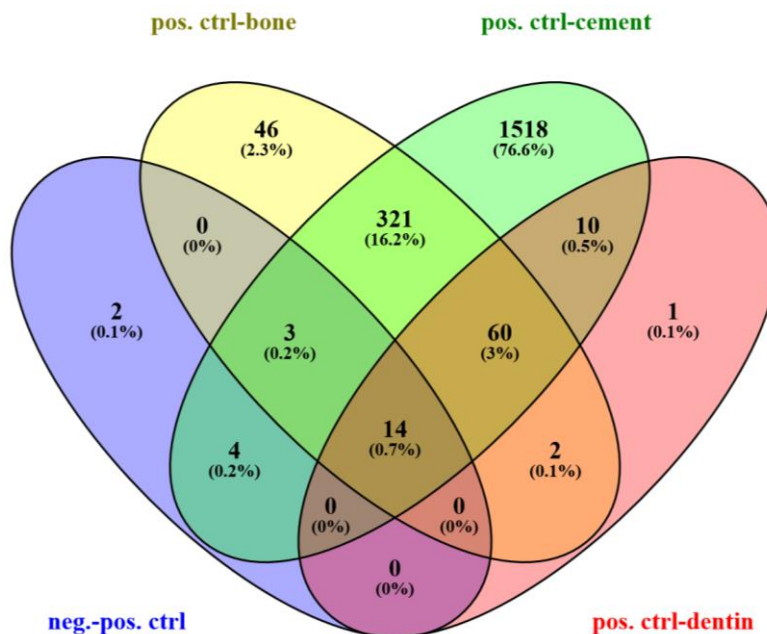


Fig. 25: Venn diagram of differentially expressed transcripts ($\log_{FC} \geq 0.5$; $P < 0.05$), demonstrating differences and similarities in the number of expressed genes between the positive control group and the other groups of the experiment.

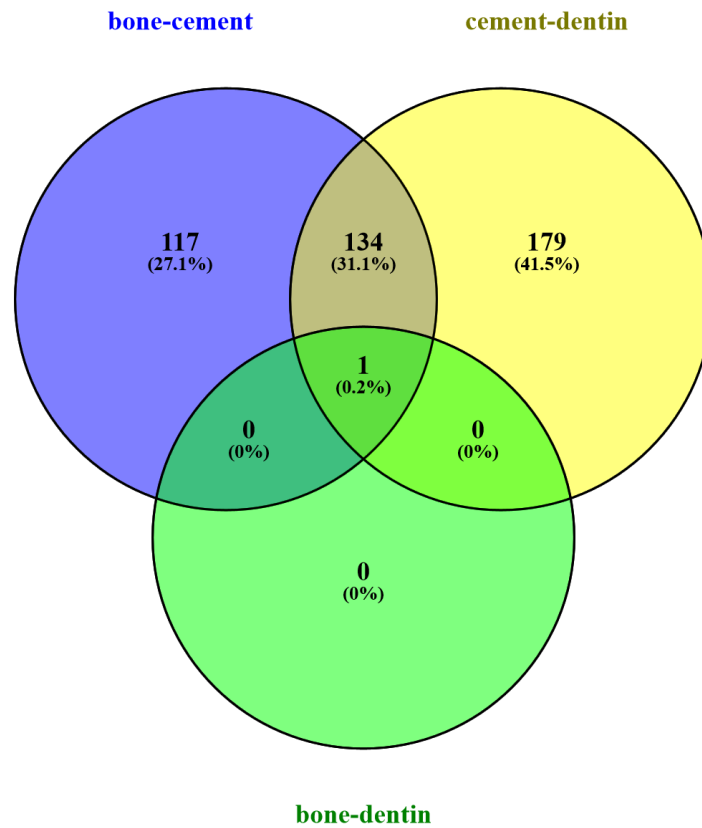


Figure 26: Venn diagram of differentially expressed transcripts ($\log_{2}FC \geq 0.5$; $P < 0.05$), demonstrating differences and similarities in the number of expressed genes between the three groups of hard tissue samples of the experiment.

3.2.2 Verification of osteoclast differentiation

Stimulation of RAW 264.7 cells with RANKL and M-CSF, in the absence of any hard tissue, induced 23 significantly differentially regulated transcripts (15 overexpressed (\uparrow) and 8 repressed (\downarrow) genes: see Fig. 27 and supplementary table S1). These genes included candidates known to be involved in osteoclast differentiation like *cxcl2*(\uparrow), inflammatory regulators like *Trib1*(\uparrow) or *Nrros*(\uparrow) and cell growth like *EGR-1*(\uparrow).

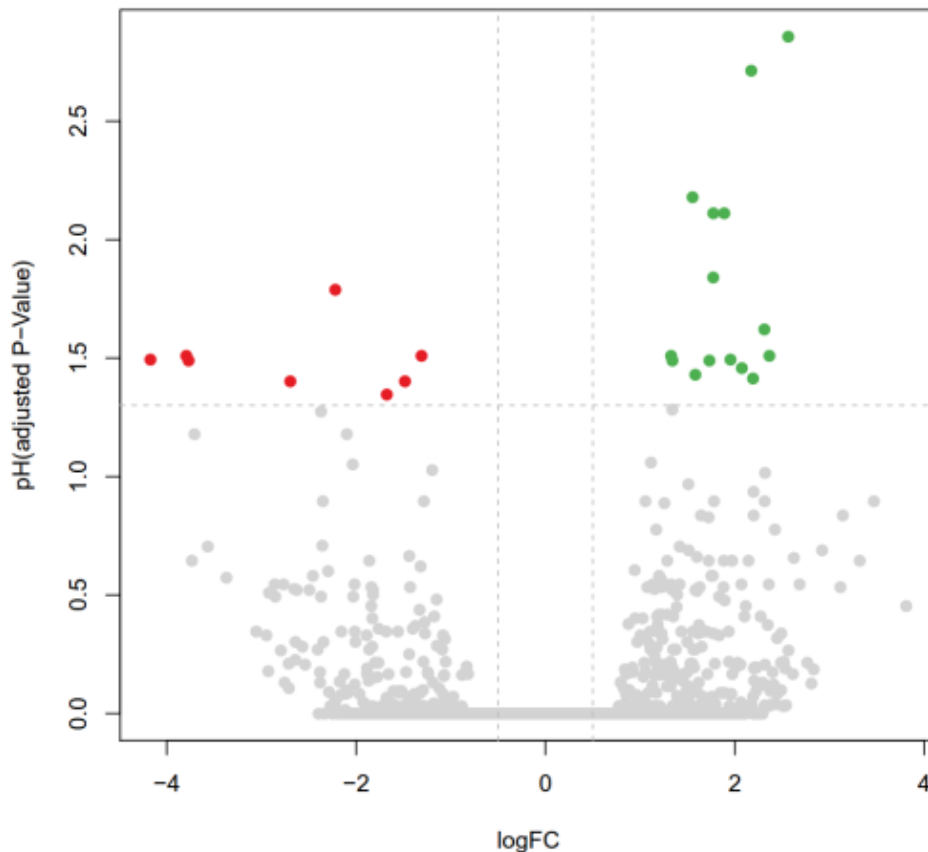


Fig. 27: Volcano plot showing the change in gene expression level after stimulating RAW264.7 cells with RANKL and M-CSF on glass. Green indicates overexpressed and red indicates repressed genes ($\log_{2}FC \geq 0.5$). Grey indicates genes that didn't show significant change in expression level. The horizontal dashed line represents a significant level of 0.05.

3.2.3 Impact of different hard tissue substrates

To identify the role of the specific hard tissue on the differentiation of the RAW 264.7 cells, a comparison of gene expression profile of the differentiated cells on plastic (positive control group) with that of the cells differentiated on the three different hard tissues was made.

The comparison between stimulated cells on bone tissue and those stimulated on glass showed 446 differentially expressed genes. (264 overexpressed (\uparrow) and 182 repressed (\downarrow) genes) (see Fig. 28 and supplementary table S2). These included typical osteoclast genes like Cathepsin K *Ctsk*(\downarrow) and genes involved in inflammatory regulation like *trib1*(\downarrow), gene

expression regulation like *Crtc2*(↑); *Rn7sk*(↑), cell growth and differentiation like *Hspa1b*(↑) or *Hspa1a*(↑).

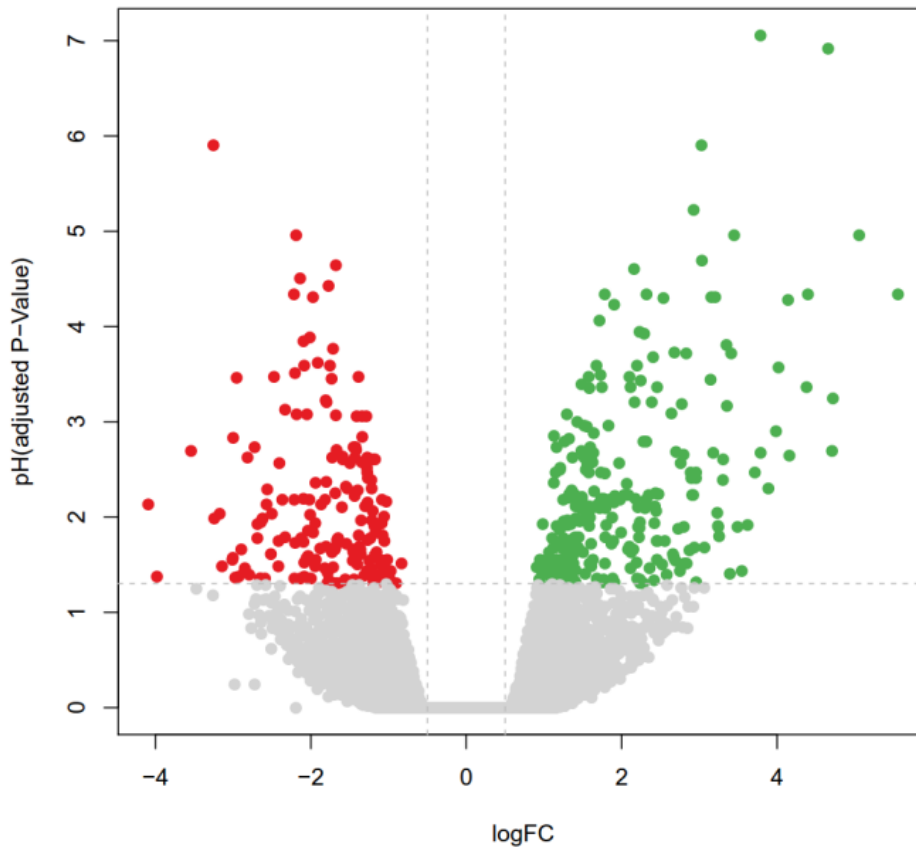


Fig. 28: Volcano plot showing the change in gene expression level after stimulating RAW264.7 cells with RANKL and M-CSF on bone tissue. Green indicates overexpressed and red indicates repressed genes ($\logFC \geq 0.5$) Grey indicates genes that didn't show significant change in expression level. The horizontal dashed line represents a significant level of 0.05.

The gene expression profile of RAW 264.7 cells stimulated on dentine demonstrated as well abundant differentially expressed genes compared to the positive control group (51 upregulated (↑) genes and 36 downregulated (↓) genes) (see Fig. 29 and supplementary table S3). Among these genes were important regulators for cell growth and differentiation like *GDF15*(↑), cell cycle and apoptosis like *GADD45Gs*(↑), differentiation regulators like *cx3cr1*(↓) and signaling pathways like *Fzd7*(↑).

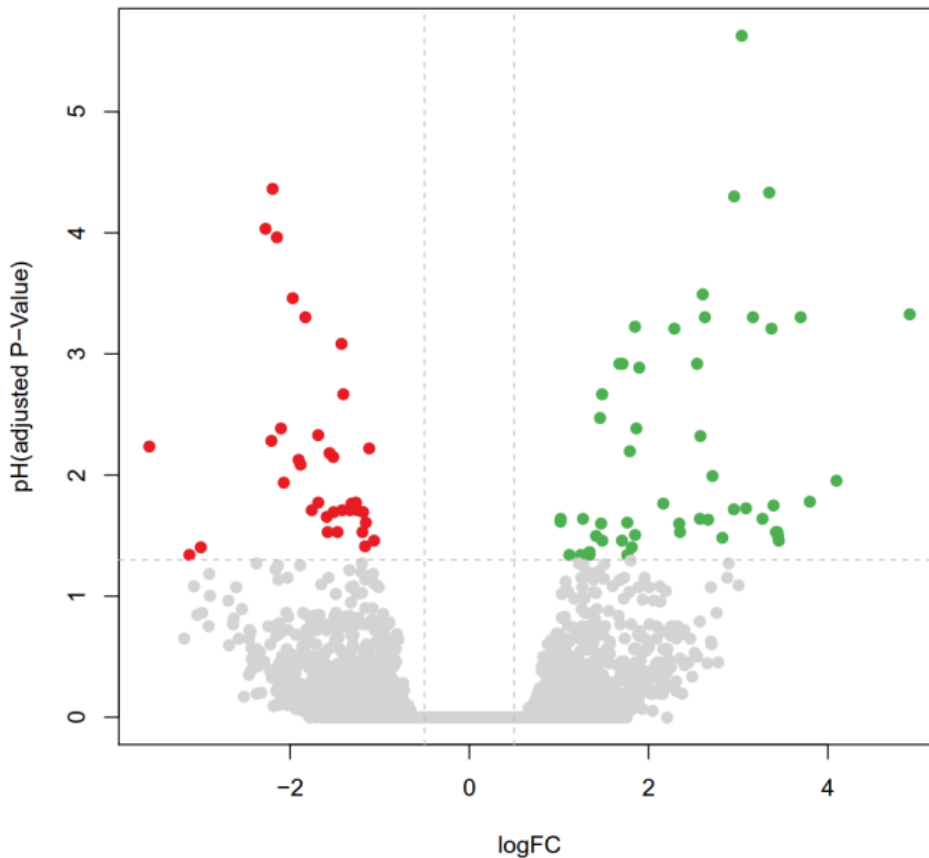


Fig. 29: Volcano plot showing the change in gene expression level after stimulating RAW264.7 cells with RANKL and M-CSF on dentine tissue. Green indicates overexpressed and red indicates repressed genes ($\log_{2}FC \geq 0.5$) Grey indicate genes that didn't show significant change in expression level. The horizontal dashed line represents a significant level of 0.05.

When comparing cells differentiated on cementum and cells differentiated on glass, there were 1930 differentially expressed genes between the two groups (899 repressed (\downarrow) and 1031 overexpressed (\uparrow)) (see Fig. 30 and supplementary table S4). These genes included differentiation regulators like *Id1*(\uparrow) and typical osteoclasts genes like *Oscar*(\downarrow), *ctsk*(\downarrow) and *Trap*(\downarrow).

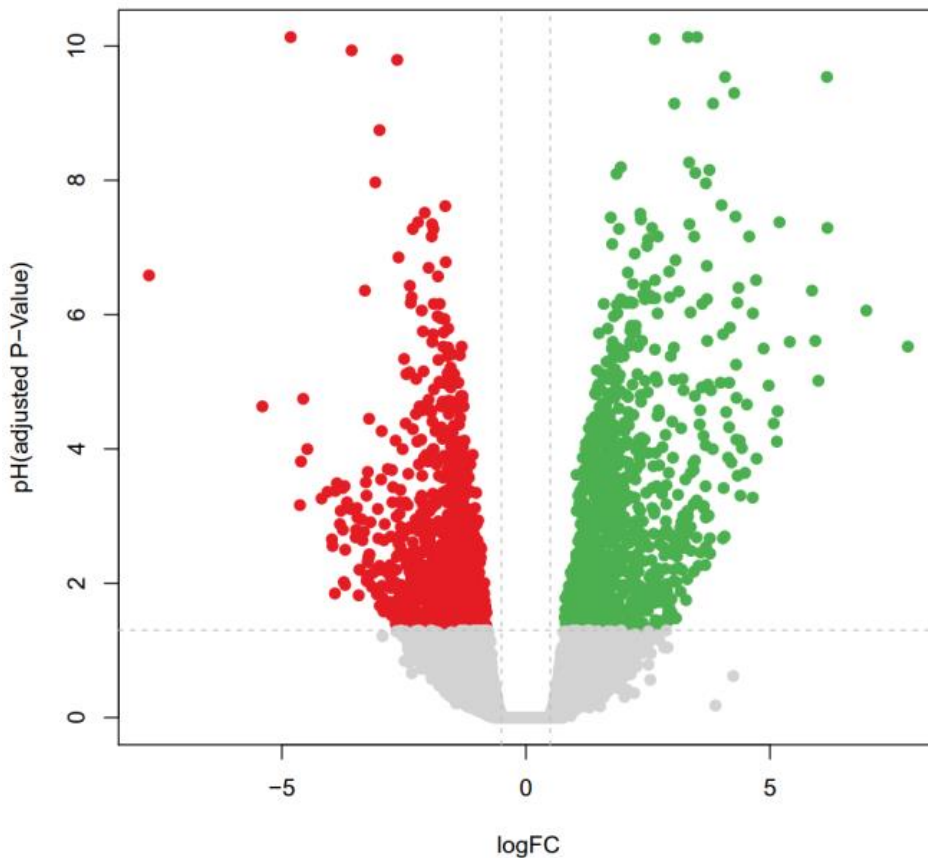


Fig. 30: Volcano plot showing the change in gene expression level after stimulating RAW264.7 cells with RANKL and M-CSF on cementum tissue. Green indicates overexpressed and red indicates repressed genes ($\log_{2}FC \geq 0.5$) Grey indicates genes that didn't show significant change in expression level. The horizontal dashed line represents a significant level of 0.05.

3.2.4 Comparison of the different substrates

Comparing the gene expressing profile of the RAW264.7 cells differentiated on the three hard tissues revealed a different behavior of the cells, depending on the specific tissue. The comparison between cementum and dentine showed 314 differentially expressed genes (186 repressed (\downarrow) and 128 overexpressed (\uparrow) in the dentine samples) (see Fig. 31 and supplementary table S5). Genes most relevant to osteoclast biology were the *Ctsk* (\uparrow) and Tartrate-resistant acid phosphatase also called acid phosphatase 5 (\uparrow). Other Genes like *Wisp1* (\uparrow) promote mesenchymal cell proliferation and osteoblastic differentiation, others are involved in cell proliferation and differentiation, e.g. : *Ndr1* (\downarrow) and *Ddit4* (\downarrow).

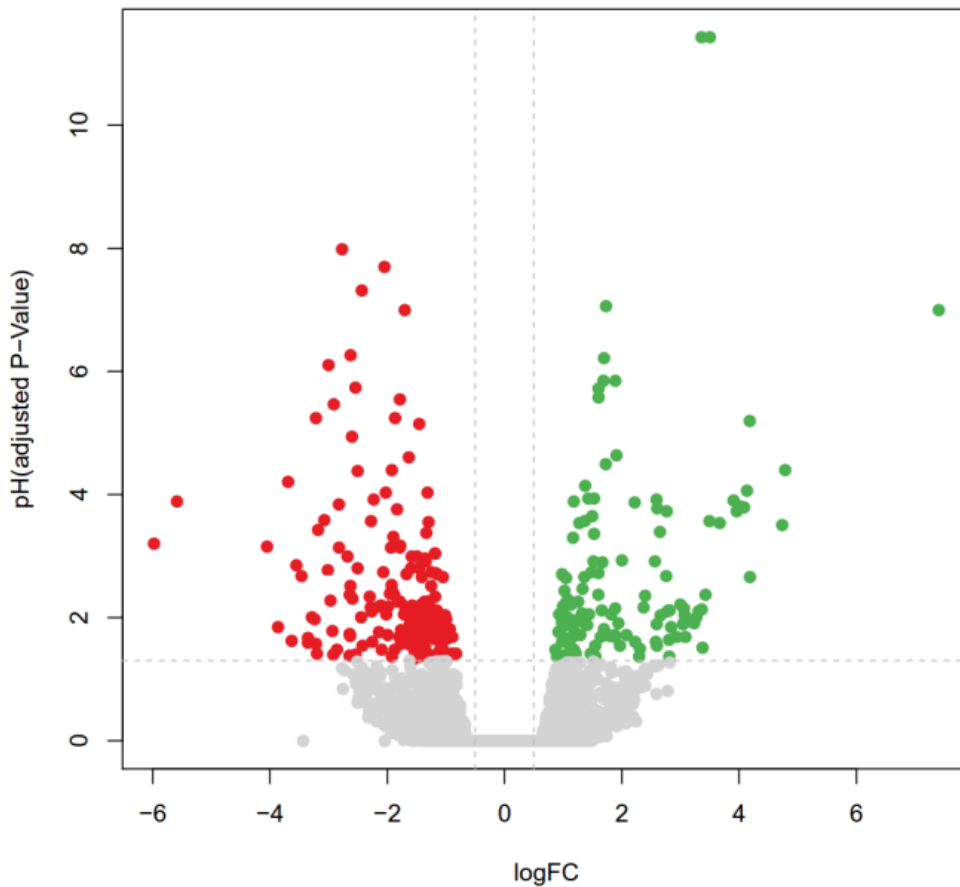


Fig. 31: Volcano plot showing the change in gene expression level in the RAW264.7 cells stimulated with RANKL and M-CSF on dentine tissue compared to RAW264.7 cells stimulated on cementum tissue. Green indicates overexpressed and red indicates repressed genes ($\log_{2}FC \geq 0.5$). Grey indicates genes that didn't show significant change in expression level. The horizontal dashed line represents a significant level of 0.05.

252 genes were differentially expressed when comparing cells grown on bone versus those on cementum (104 repressed (\downarrow) and 148 overexpressed (\uparrow) in the cementum samples) (see Fig. 32 and supplementary table S6). Among them were some important genes known to be involved in osteoclast growth and differentiation like *Nfatc1*(\downarrow) and *Src*(\downarrow) as well as genes related to the activity of the osteoclasts like *Acp5*(\downarrow), *Ctsk*(\downarrow), and *OSCAR*(\downarrow).

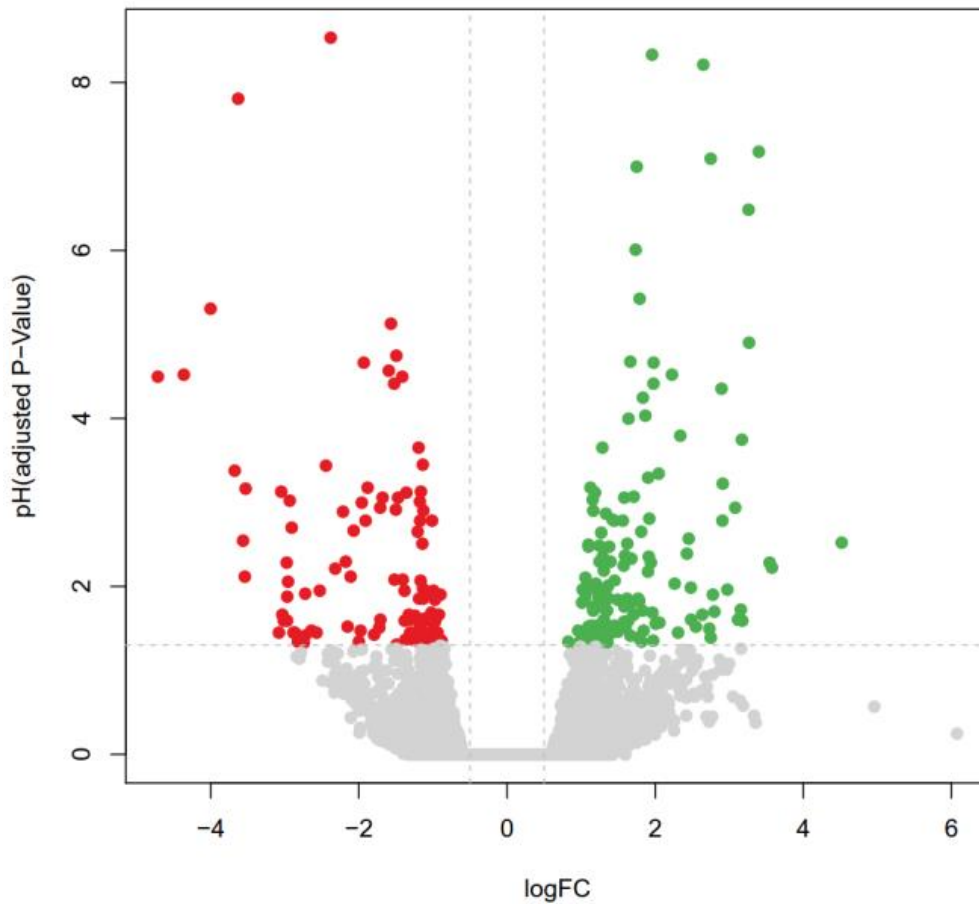


Fig. 32: Volcano plot showing the change in gene expression level in the RAW264.7 cells stimulated with RANKL and M-CSF on cementum tissue compared to RAW264.7 cells stimulated on bone tissue. Green indicates overexpressed and red indicates repressed genes ($\log_{2}FC \geq 0.5$) Grey indicates genes that didn't show significant change in expression level. The horizontal dashed line represents a significant level of 0.05.

Interestingly, as bone and dentine samples were compared, there was only one differentially expressed gene, which is Cathepsin K (\uparrow) and it was upregulated by 3.8 folds in dentine samples. (see Fig. 33 and supplementary table S7).

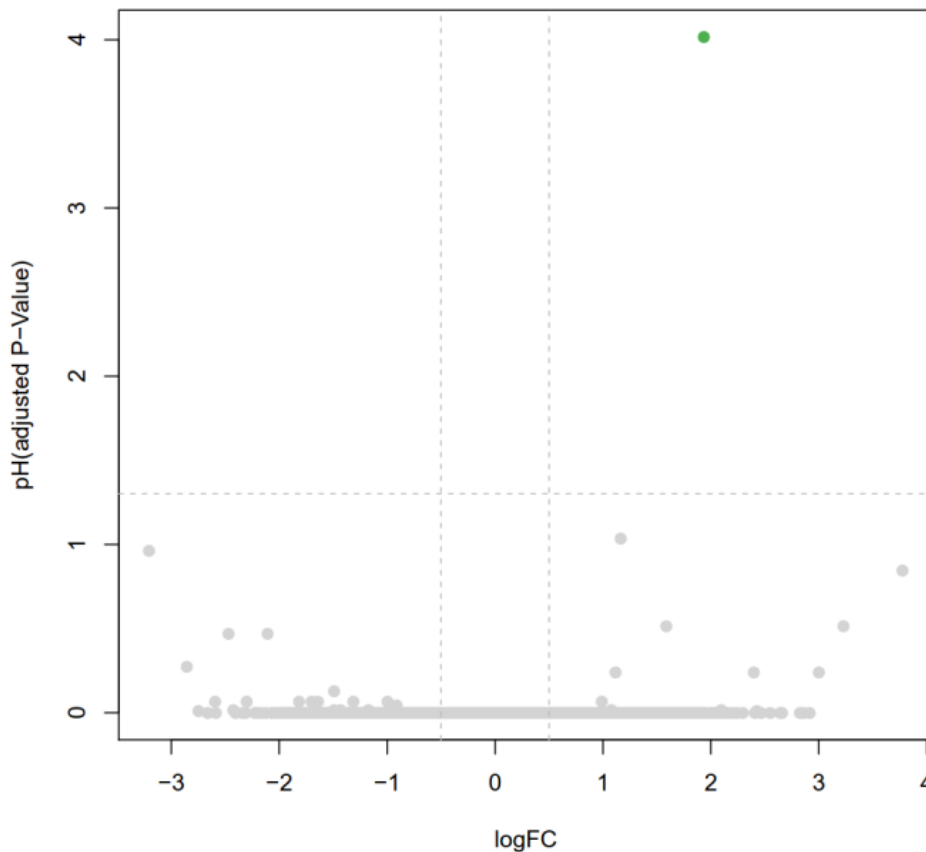


Fig. 33: Volcano plot showing the change in gene expression level in the RAW264.7 cells stimulated with RANKL and M-CSF on dentine tissue compared to RAW264.7 cells stimulated on bone tissue. Green indicates overexpressed genes ($\log_{2}FC \geq 0.5$) Grey indicates genes that didn't show significant change in expression level. The horizontal dashed line represents a significant level of 0.05.

3.2.5 Hierarchical cluster analysis

To show the similarity in the expression level of the top 50 regulated genes between the samples, hierarchical clustering was used to group similar expression level into clusters. The resulting hierarchy of clusters is displayed in a tree-form shape called dendrogram. The gene clusters show similarity between the unstimulated cells and cells stimulated on glass as well as similarity between bone and dentin samples. A colored representation of the data in form of a heat map, representing the differential expression of 50 genes, and the dendrograms are shown in Fig. 34.



Fig. 34: Heat map showing the top 50 regulated transcripts in RAW264.7 cells for the five groups of the sample. The low expression value is colored in blue and the high expression value is in red. Rows represent the genes and are labeled with the gene symbol and columns represent the samples. The sample legend on the right-hand of the heat map indicates which color correspond to which group. The dendrogram on the left-hand side shows clustering of samples as rows and the dendrogram on the top shows clustering of samples as columns.

3.2.6 Results of Ingenuity pathway analysis

According to IPA, a total of 266 canonical pathways were activated in bone samples compared with positive control samples, 392 canonical pathways were activated in dentine samples compared with positive control samples and 359 canonical pathways were activated in cementum samples compared with the positive control samples (supplementary tables supp.Tab.8-supp.Tab.10 and supplement figures supp.Fig.1-supp.Fig.3). The comparison between the RAW264.7 cells differentiated on the three hard tissues showed 348 activated canonical pathways in dentine samples compared to bone samples, 435 activated canonical pathways in cementum samples compared with bone samples and a total of 407 canonical pathways were activated in dentine samples compared with bone samples (supplementary tables supp.Tab.11-supp.Tab.13 and supplement figures supp.Fig.4-supp. Fig.6). Pathway networks between each comparison group mentioned above are demonstrated in supplement figures (supp.Fig.7- supp.Fig.12) and supplement tables (supp.Tab.14-supp.Tab.19). Since the corresponding supplements are very extensive, an imprint in this work has been omitted. The supplements can be requested at any time by the author or the doctorate supervisor (Prof. Dr. Jäger).

4. Discussion

4.1 Discussing the morphological results

At the begin of this study the fusion process of mononuclear RAW264.7 cells to form multinucleated cells, which was induced by the cytokines M-CSF and RANKL, was verified. After three days of incubation, extensions from the cells and by the end of the incubation time (12 days), multi nucleated cells were seen. The formation of the multi-nucleated giant cells was observed in both samples, but with the 50,000 cells sample, the fusion was obviously facilitated because of the higher density of cells, which resulted in more multinucleated cells.

Toluidine blue staining was performed to identify the resorption pits initiated by the differentiated RAW264.7 cells. These resorption pits demonstrate the ability of the differentiated RAW264.7 cells to resorb hard tissue.

In addition, samples were prepared and examined using the scanning electron microscope, to visualize the morphological changes on dentine discs after differentiating the RAW264.7 cells. Osteoclast-like cells with extensions and podosomes were observed. Long resorbing trenches which correspond to continuous resorption were observed (Merrild et al., 2015).

Thus, M-CSF and RANKL cytokines were reliable to differentiate the RAW264.7 cells into multinucleated resorbing cells. Many studies showed the importance of M-CSF gene osteoclast recruitment and survival (Sanuki et al., 2010; Falkenberg et al., 1990).

As seen in figures 3.1 and 3.2 a lot of the cells were not in contact with the dentine slices, which means that most of the cells were not in the position to resorb the dentine tissue. Thus, using these cells to isolate RNA and to study differential gene expression during resorption of different hard tissues will not be reliable.

In order to increase the contact surface between the cells and the hard tissues it was decided to prepare powder from the hard tissues, namely from bone, dentin and cementum.

To the best knowledge this study is the first one to use the different tooth hard tissues in form of powder, especially cementum because of the difficulty of preparing study samples from this hard tissue.

To confirm the differentiation of the RAW264.7 cells into osteoclast-like cells, three hard tissue powder samples were prepared and the RAW264.7 cells were cultured on them. Cells were stimulated with RANKL and M-CSF for 12 days and then stained with TRAP. The hard tissue particles were identified with many TRAP positive osteoclast-like cells in all three powder samples. Interestingly, the cells in the hard tissue samples looked bigger with 4-5 nuclei and had more extensions.

4.2 Discussing the differentially gene expression levels

The main goals of RNA-Seq are to identify the gene sequence (the particular order of A, C, G, U), gene structure (i.e. intron-exon junctions or 5', 3' untranslated regions) and the abundance of specific RNA molecules in a chosen sample. Abundance means the numerical amounts of each sequence. Once the sequence and gene structure have been elucidated, abundance values can be attributed to each gene as well as various features in their structures, which makes it possible to make comparative studies between healthy versus sick samples, non-treated versus treated or time point 0 versus time point 1 in different samples.

Differential expression (DE) analysis is one of the reliable features of RNA-Seq. DE refers to the identification of genes that are expressed in significantly different quantities in distinct samples. In our study we used this analysis to make three main comparisons. Firstly, between the stimulated and unstimulated RAW264.7 cells to identify the genomic features of the differentiating osteoclast-like cells. Secondly, between the cells differentiating on glass and the cells differentiating on three different hard tissues. The last comparisons were made to study the influence of the specific hard tissues on the differentiated osteoclast-like cells at transcriptomic level.

4.2.1 Differential gene expression level during RAW264.7 cells differentiation

Comparison of unstimulated RAW264.7 cells and those stimulated on glass revealed 23 significantly differentially regulated genes (15 overexpressed \uparrow and 8 repressed \downarrow). The highest increase was detected for Trib1 (tribbles pseudokinase 1) (5.9 \uparrow). According to Satoh et al., Trib1 is critical for macrophages differentiation (Satoh et al., 2013). To the best knowledge, the association between trib1 and osteoclast differentiation was not addressed before but taking into consideration that osteoclasts are the most characterized type of multinucleated giant cells which are formed by fusion of multiple macrophages, an involvement of Trib1 in osteoclasts differentiation seems reasonable.

C-X-C Motif Chemokine Ligand 2 or Cxcl2 was also significantly increased (5.2 \uparrow). This gene is involved in osteoclasts differentiation (Dapunt et al., 2014). A study done by Jeongim et al. (2010), showed also a 4-fold induction of cxcl2 after stimulation of RAW264.7 cells with RANKL and M-CSF, which verifies the role of this gene in the differentiation of osteoclasts.

Among the other upregulated genes was the Negative regulator of reactive oxygen species (Nrros) (3.4 \uparrow). This was also observed by Kim et al. (2015), as Nrros gradually upregulated during the first three days during RANKL-induced osteoclastogenesis.

Further on, Early growth response 1 (EGR1), was mentioned as a main player in the regulation of cell growth and differentiation (Liu et al., 1998). It was upregulated by 4.9 folds in the cells differentiated on glass.

Another interesting gene is the transcription factor MafB, which was upregulated by 2.5 folds after stimulation. A previous study by Kim et al. (2007), showed that MafB negatively regulated RANKL-induced osteoclast differentiation from bone marrow-derived monocyte/macrophage lineage cells (BMMs) and reported that expression levels of MafB were significantly reduced by RANKL during osteoclastogenesis which differs from our findings.

On the other hand, some genes were significantly downregulated, for example Heat shock protein 8 (Hspa8) by 2.7 folds. This gene was described by Hart et al. (2004), as a contributor to biological processes like cell growth and differentiation. An association

between Hspa8 expression and osteoclasts differentiation was mentioned in a recent study by Notsu et al. (2016). They stated that knockdown of HSPA8 strongly inhibited RANKL-induced osteoclastogenesis from RAW264.7 macrophage-like cells which coincides with our findings.

Comparing the expression level of the previously mentioned genes in unstimulated cells with those in stimulated cells on the three different hard tissues didn't show any statistically significant change in expression level in neither of the three hard tissues except for transcriptional factor Mafk, which was upregulated by 7.5 folds in the cells stimulated on cementum.

Otherwise, divers genes were differentially expressed in the hard-tissue groups during the differentiation of the RAW264.7 cells, like Insulin-like growth factor 1 (IGF-1) which was upregulated in the three hard-tissue samples by 2.9 folds in the bone samples, 3.6 folds in the dentine samples and 4 folds in the cementum samples. IGF1 is involved in various cellular processes including differentiation and morphogenesis. Wang et al. (2006) showed that IGF1 regulates osteoclastogenesis by promoting their differentiation and IGF-I deficiency impaired osteoclastogenesis. The expression level change of this gene wasn't statistically significant in the absence of mineralized hard tissues.

Growth differentiation factor 15 (GDF15) was also upregulated in the three hard tissue groups as following: 7.7 in the bone samples, 10.5 folds in the cementum samples and 3.5 folds in the dentine samples. GDF15 belongs to transforming growth factor beta superfamily. It is upregulated in most organs following injury and seems to have a role in regulating inflammatory pathways, apoptosis, cell repair and cell growth. A study done by Westhrin et al. (2015), showed that GDF15 increased osteoclasts differentiation and at the same time inhibited osteoblasts differentiation in vitro.

FZD7 gene is a receptor for wnt signaling proteins. It was upregulated by 16.3 folds in the cementum samples and by 4.1 folds in the bone samples but there wasn't any statistical significance in the expression level between unstimulated cells and stimulated cells in the dentine group. According to Weivoda et al. (2015), wnt signaling proteins reduce osteoclast formation and activate osteoblast formation.

One most interesting gene was the inhibitor of differentiation 1 or ID1. The Ids family is responsible for a negative regulation of RANKL induced osteoclastogenesis (Lee et al., 2006). In this study, Id1 was downregulated after stimulation with RANKL but without statistical significance compared with unstimulated cells. In contrast, it was significantly upregulated by 7.4 folds in the cementum samples.

Heat shock 70kDa protein 1B, also known as HSPA1B was markedly upregulated in the cementum samples by 43 folds but in the other two samples the differential gene expression wasn't statistically significant compared to the unstimulated cells. Its function contributes to biological processes including signal transduction, apoptosis, protein homeostasis, cell growth and differentiation (Mayer and Bukau, 2005). Hart et al. (2004) mentioned the correlation of this gene with the alveolar bone loss in periodontal disease, as they detected an over expression of Hspa1b in osteoclasts.

Of major interest was the downregulation of typical osteoclast genes like Cathepsin K (Ctsk) and Tartrate-resistant acid phosphatase (TRAP) or Acid phosphatase 5 (Acp5) in the cementum samples by 5 folds for Ctsk and by 4.3 for Acp5 in comparison with unstimulated cells. Cathepsin K is an enzyme encoded in humans by the Ctsk gene (Inaoka et al., 1995). The lysosomal cysteine protease is involved in bone remodeling and resorption. It is induced during osteoclast precursors differentiation after stimulation with RANKL and M-CSF. Cathepsin K functions by degrading the organic components of the bone matrix and is critical for osteoclastic bone resorption. Because of that it is considered to be the most important proteases in osteoclasts (Li et al., 1995). TRAP or Acp5 serves as a biochemical marker for osteoclast function because of its expression by osteoclasts, macrophages, dendritic cells and several other cell types. It can degrade bone matrix proteins including osteopontin (OPN) and integrin binding sialoprotein (IBSP) and has a critical role in many biological processes including collagen synthesis and degradation, cytokine production by macrophages and macrophage recruitment (Hayman, 2008). Overexpression of Acp5 resulted in enhanced bone turnover and a mild osteoporotic phenotype (Angel et al., 2000).

The differential gene expression of the described genes is indicative for the hypothesis that the mineralized hard tissues in contact with cells influences the RANKL-induced osteoclastogenesis from RAW264.7 cells.

Next, in order to figure out the impact of the specific type of mineralized hard tissue on the resorption activity of the differentiated osteoclast-like cells, we compared the differentiated RAW264.7 cells on glass (positive control group) with the differentiated cells on the three different hard tissue powders samples and the relevant genes with significant differential gene expression are mentioned below :

Nrros gene was downregulated in all three samples compared with differentiated cells on glass, that is by 1.9 folds in the bone samples, 1.8 in the dentine samples and 2.1 in the cementum samples. Otherwise, Cxcl2 gene was downregulated only on the cementum samples by 2.1 folds. In the other two groups there wasn't any significant difference in the gene expression level of this gene. In the same manner, downregulation of typical osteoclast genes was recognized. For example, Ctsk was downregulated by 3.2 folds in the bone samples and in the cementum samples by 4.8 folds but in the dentin groups there wasn't any significant difference in gene expression. Also, Asp5 gene was only significantly downregulated in the cementum samples by 3.5 folds. Of interest was the repression of the OSCAR gene in the cementum samples. This osteoclast-associated receptor gene (OSCAR) was mentioned to be upregulated during osteoclast differentiation (Jung et al., 2008) and its expression has been associated with both bone loss and inflammation in human diseases (Humphrey and Nakamura, 2016). The differential gene expression of this gene wasn't statistically significant in the bone and dentine samples but was significantly repressed in the cementum samples by 2.4 folds.

The repression of the previously mentioned genes may reflect a possible negative regulatory role of the hard tissues, especially of the cementum, controlling the activity of the resorbing cells by altering the expression of some specific genes.

In contrast to the upregulation of the Trib1 gene during differentiation of the RAW264.7 cells cultured on glass, this gene was downregulated in the three hard tissue samples by 2.2 folds in the bone and cementum samples and by 1.8 in the dentine samples.

On the other hand, some other genes were significantly upregulated as follows:

Mafb gene was upregulated by 2.9 folds just in the cementum samples. In the same way, Hspa8 gene was upregulated in the bone, dentin and cementum samples by 9.2, 5.8 and 13.1 respectively.

Unlike the upregulation of the IGF1 gene during the differentiation of RAW264.7 cells on the three hard-tissue samples, this gene was only significantly upregulated on cementum samples when compared with the differentiated RAW264.7 cells by just 1.8 folds. A study done by Götz et al. (2008), investigated the role of this gene in tooth movement, root resorption and repair by immunohistochemistry and they confirmed the involvement of IGF1 not only in resorption processes and clastic activities but also in the resorption-repair sequence, which was considered to be a coupling process as known from bone.

Growth differentiation factor 15 (GDF15) was again significantly upregulated in all three hard-tissue samples, by 8.1 folds in bone samples, 3.7 folds in the dentine samples and 11.1 in the cementum samples. We mentioned previously of the study done by Westhrin et al. (2015), which revealed the simultaneous role of GDF15 in osteoclast differentiation and osteoblast inhibition in vitro. Therefore, GDF15 may have a role in uncoupling cementum or dentine formation and resorption.

The FZD7 gene is part of the frizzled gene family which encodes the wnt signaling proteins. The upregulation of this gene in the bone and cementum samples was demonstrated again when compared with the cells differentiated on glass by 4.8 folds in the bone group and 19.6 in cementum group. Of interest was the upregulation of this gene in the dentin group by 3.4 folds that wasn't seen in the previous comparison with undifferentiated cells. This upregulation might be relevant to the coupling between resorption and regeneration.

Again Id1, or Inhibitor of differentiation 1 gene, showed a statistically significant increase in gene expression level only in the cementum samples, and was upregulated by 11.3 folds. This observation could support the idea of the regulatory effect of the dental cementum on the resorbing osteoclast-like cells. Chan et al. (2009), revealed in their study that a loss of Id1 increased the expression of typical osteoclasts genes like Oscar, TRAP and Ctsk.

Hspa1b was the most upregulated gene in the cementum samples by 226.9 folds and unlike the comparison with the negative control group, this gene was also upregulated by 33.2 folds in bone samples and by 3.6 in dentin samples in comparison with the positive

control group, which may reflect an important role of this gene in the resorption process of the mineralized dental root tissues.

The comparison between the cells differentiated on glass (positive group) and the cells differentiated on the three different mineralized hard tissue revealed also some genes with a significant change of expression levels that were specific for this comparison. This means that the differential gene expression of these genes wasn't observed in the comparison with the undifferentiated RAW264.7 cells. Some of these genes are mentioned below:

The Hyaluronidase 1 (Hyal1) gene was upregulated by 3.7 folds in the bone samples, 3.2 in the dentin samples and by 4.3 in the cementum samples. This gene encodes the hyaluronidase enzyme which is able to degrade hyaluronic acid which is one of the major glycosaminoglycans of the extracellular matrix, and is involved in cell proliferation, migration and differentiation (Stern, 2003). A recent study by Puissant and Boonen (2016) showed upregulation of this gene in RAW264.7 cells stimulated with RANKL and this finding pointed out the involvement of Hyal1 in bone metabolism and perhaps bone remodeling.

The *Cx3cr1* gene encodes chemokine receptor 1. This gene was downregulated in the dentine and cementum samples by 1.5 and 1.4 respectively and didn't show any significant difference in the expression level in the bone samples. According to Koizumi et al. (2009), this chemokine regulates the differentiation and function of osteoclasts. It is expressed by osteoclasts as a receptor for *Cx3cl1* that is to be expressed by osteoblast to induce differentiation of osteoclasts.

The *Nlrp3* gene provides instructions for the coding protein family called nucleotide-binding domain and leucine-rich repeat containing (NLR) proteins. This gene was downregulated by 2.1 folds in the dentine group and by 2.3 folds in the cementum group. In contrary, the expression level wasn't significantly changed in the bone group. The *Nlrp3* gene is expressed predominantly in macrophages as a component of the inflammasome, which is a protein complex responsible for the activation of the inflammatory response through secretion of pro-inflammatory cytokines like interleukin-1 β (IL-1 β) and interleukin 18 (IL-18) (Martinon et al., 2002). A recent study by Alippe et al. (2017), showed that

products originating from bone matrix activate the expression of Nlrp3 in osteoclasts which further amplifies the bone resorption.

The cluster of differentiation 47 gene or CD47 is also known as Integrin associated protein. In our study this gene was significantly upregulated by 1.8 folds only in the cementum samples compared to the RAW264.7 cells differentiated on glass. Koskinen et al. (2013) concluded that a lack of CD47 impairs osteoblast differentiation and causes reduced formation of osteoclasts. In a different study, Willingham et al. (2012) mentioned that CD47 is a “don't eat me” signal for phagocytic cells and is expressed on the surface of all human solid tumor cells. They showed its function to block phagocytosis and that blockade of its function leads to tumor cell phagocytosis and elimination. This result validated CD47 as a target for cancer therapy. If this gene has a role in the cementum biology and dental root resorption is not yet known but might be interesting to investigate.

One of the advantages of the applied method of RNA-sequencing over conventional microarray analysis is that RNA-Seq enables the identification of non-coding differentially expressed genes. As an example for non-coding genes the Rn7sk gene is to be mentioned. The involvement of this gene in regulating transcription was mentioned by Peterlin et al. (2012). To our knowledge, the role of this non-coding gene in osteoclasts differentiation or resorption activity wasn't mentioned before. In this study this gene was upregulated by 10.9, 6.2 and 72.4 folds in bone, dentine and cementum respectively compared with the cells differentiated on glass.

The last comparison was set up to evaluate possible differences between the hard-tissue samples themselves in order to investigate the reaction of the differentiated osteoclast-like cells on these three different hard tissues, in terms of differential gene expression.

Comparing bone and dentine samples showed differential expression level of only one gene that was Cathepsin K (Ctsk) which was upregulated by 3.8 folds in the dentine samples. This result could be explained by the structural similarities between these two hard tissues. The total inorganic component of dentin is 70% in weight and organic components represent 20% which is similar to bone composition with 65% inorganic components and 25% organic components (Naqshbandi et al., 2013).

When comparing cells differentiated on bone versus cementum, typical osteoclasts genes were significantly downregulated in the cementum group. For example, *ctsk* was downregulated by 1.5 folds, *Acp5* was downregulated by 2.3 folds and *OSCAR* was downregulated by 2.5 folds. On the other hand, significant upregulation of some interesting genes was noticed in the cementum group like the inhibitor of differentiation gene (*Id1*) which was upregulated by 3.5 folds. The *Fzd7* gene was upregulated by 4 folds and the *Mafb* gene that was upregulated by 3.4 folds. Also, the non-coding gene *Rn7sk* was upregulated by 6.6 folds.

Of special interest was the differential expression level of the genes mentioned above as cementum and dentin groups were compared. *Ctsk* and *Acp5* were upregulated in the dentine samples by 11.3 and 10.2 folds respectively. *OSCAR* gene didn't show a statistically significant difference in the expression level. Otherwise, the *Id1* gene was by 2.7 folds downregulated in the dentine samples as well as the *Fzd7* gene by 2.5 folds. Likewise, was the *Mafb* gene downregulated by 1.7 folds and *Rn7sk* by 3.5 folds. This differences in gene expression level could be due to the different structural composition of the dental cementum which consists of about 45% to 50% inorganic material by weight, mainly hydroxyapatite, and 50% to 55% organic material by weight, mainly collagen, extra cellular matrix proteins and water (Yamamoto et al., 2016).

Because of the huge number of the differentially activated canonical pathways between the groups of the study and their related networks, the results of the IP analysis might be useful for further studies towards enhancing our understanding of the interaction between the clast cells and the different types of hard tissues.

Taken together, the experiments showed many differences in gene expression level between all groups of our study. Thus, a possible influence of the mineralized tissues, as one of the environmental factors, on the differentiation and activity of osteoclast-like cells is supported.

Like for microarray analysis, validating the differentially expressed genes identified using RNA-sequencing experiments is important to confirm the biological conclusions. The differentially expressed genes are often validated using quantitative reverse transcriptase polymerase chain reaction (RT-PCR) (Fang and Cui, 2011). In order to consider the DGE

as a true-positive, both RNA-seq and RT-PCR should show the same direction (upregulation or down-regulation) of differential expression for the gene of interest, also the fold changes estimated from RNA-seq should have a high correlation with that from the RT-PCR. Thus, a further study to confirm the differential expression of some of the previously mentioned genes using RT-PCR is suggested. Moreover, this study focused on the genomic aspect of the osteoclast-like cells, but in order to gain a complete understanding of this cellular system, a further investigation at a proteomic level is recommended. This is particularly important as the cells continually communicate with their surroundings by the secretion of biomolecules like proteins and peptides which end up in the extracellular medium and might indicate a specific physiological or pathological process (Finoulst et al., 2011). One of the common methods to study proteins are immunoassays or protein detection with antibodies. The enzyme-linked immunosorbent assay (ELISA) and Western blot are two antibody-dependent techniques that might be used for detection and quantification of individual proteins. Depending on the results of this study, Western blot or ELISA tests could be used to detect and quantify specific proteins which might be released in the culture medium (supernatant) of the RAW264.7 cells during differentiation and the resorption process.

There is an ongoing discussion about the possible intracellular mechanisms that might be involved in the apparent ability of osteoclasts to “sense” the kind of substrate that they are going to resorb. Osteoclastic resorption is a process requiring physical close contact between the resorbing cell and the bone matrix. Many authors hypothesized that the recognition of different substrates by osteoclasts is triggered by the interaction of $\alpha\nu\beta3$ integrins on the osteoclasts and proteins of the extracellular matrix (ECM) of the hard tissue to be resorbed (Faccio et al., 2003; Fuller et al., 2010). It was demonstrated that $\alpha\nu\beta3$ integrin plays a role in the initial adhesion of osteoclasts to their substrates (Nesbitt et al., 1993, Duong et al. 2000). Rat osteoclasts adhere in an $\alpha\nu\beta3$ -dependent manner to ECM proteins containing so called RGD sequences which represent tripeptides consisting of the amino acids Arginine, Glycine, and Aspartate. Typical ECM proteins containing the RGD sequence are vitronectin, osteopontin or bone sialoprotein. (Helfrich et al, 1992). In addition, osteoclastic bone resorption was partially inhibited by both anti- $\alpha2$ and anti- $\beta1$ antibodies (Nakamura et al., 1996). Thus, recognition of extracellular matrix components by osteoclasts is supposed to be an important step in initiating osteoclast function.

Concerning the three hard tissues under investigation, several studies compared the composition of bone, dentin and root cementum with respect to the prevalence of different ECM proteins. Typically, the ECM consists of collagen fibers that form a matrix for the deposition of the carbonate apatite crystals. In addition, a number of other proteins and proteoglycans collectively referred to as non-collagenous proteins (NCPs) can be found. Some NCPs were found exclusively in dentin, and were exclusively expressed by odontoblasts (Butler and Ritchie, 1995). Only three proteins are considered to be dentin specific: dentin phosphoprotein (DPP), Dentin matrix acidic phosphoprotein 1 (Dmp1) and dentin sialoprotein (DSP). Another group of ECM protein can be found in all hard tissues and is synthesized by the tissue specific cells. Examples are bone sialoprotein (BSP) and osteocalcin (bone Gla protein, BGP) (Butler and Ritchie, 1995). In addition, dentin contains molecules secreted by specifically odontoblasts which are also synthesized by diverse cell types and are found in the ECM of many other tissues, including different hard and soft tissues. Examples for this group include osteopontin and osteonectin (Butler and Ritchie, 1995).

Although bone and root cementum share similarities in morphology and matrix composition it is well established that each matrix contains unique proteins that may be responsible for their physiologic differences. For both tissues, type I collagen is the primary ECM component, with the remaining organic matrix being composed of varying amounts of noncollagenous proteins (NCPs). These include proteoglycans (e.g., versican, decorin, and biglycan), glycoproteins (e.g., osteonectin and arginine-glycine-aspartic acid (RGD) integrin-binding proteins), and gamma-carboxyglutamic acid (gla)-containing proteins (e.g., matrix gla protein, protein S, and osteocalcin).

Applying the method of proteomics, Salomon et al. (2013) demonstrated that a total number of 318 proteins were identified when comparing alveolar bone and root cementum tissues. On the other hand, in addition to shared proteins between these tissues, 105 and 83 proteins were identified exclusively for bone or root cementum, respectively.

Possible relevance for the clinic:

The process of hard tissue resorption requires specific interaction between various cells and hard tissues, whether being bone, cementum or dentine. As an example, identifying specific genes involved in root cementum resorption could be a way for the early detection of root resorption in patients undergoing orthodontic treatment. Targeting specific genes that stimulate cementum / dentine resorption without inhibiting the bone metabolism or in contrary amplifying other genes in order to accelerate tooth movement without threatening the dental root tissues might then be possible.

Nowadays, orthodontists are embracing the concept of personalized medicine and are following the development of an expanding list of tests capable of revealing significant information about the biological profile of each individual patient which may facilitate the individualization of diagnosis, treatment planning and risk assessment for every orthodontic patient. The Term “personalized orthodontics” was mentioned for the first time in 2008, a paper used this term in relation to genetic evaluation of the patient and outlined future scenarios in orthodontic practice (Hartsfield and James, 2008).

In this study, a step toward defining the regulators of dental root resorption was made and many areas of uncertainty that warrant further study and investigation were opened.

5. Summary

Hard tissue resorption is a multistep process, which requires a complex interaction between multinucleated clast cells and the hard tissues to be resorbed. This process is regulated by genetic factors and inflammatory cytokines. This study was directed toward the clast cells to clarify the ability of these cells to distinguish between the resorbed substrates and the possible influence of the resorbed tissues on the intracellular mechanism behind the resorption and repair process. To study the influence of the mineralized tissues on the differentiation and activity of the clast cells, RAW264.7 cells were cultured on powder substrates made from bone, dentine and cementum tissues. The cells were stimulated with RANKL and M-CSF for 12 days then RNA was isolated and gene expression induced by the three hard tissues was investigated using a transcriptome wide approach. Gene expression analysis was performed based on RNA-Sequencing. The results showed many differentially expressed gene between the samples of the study. 1930 genes were significantly differentially regulated on cementum compared with the cells stimulated on glass (as positive control group), 446 between bone tissue and the positive control 87 between dentin and the positive control. Moreover, the comparison between the stimulated cells on the hard tissues showed 314 differentially regulated genes between cementum and dentine, 252 between bone and cementum and just one significantly differentially regulated gene between dentine and bone. These results reflect the influence of the hard substrates on the differentiation and activity of osteoclast-like cells. For example, *ctsk* is one of the well-known genes involved in the mineralized tissue resorption process. This gene was downregulated by 3.2 folds in the bone samples and in the cementum samples by 4.8 folds compared to the cells differentiated on glass but in the dentin groups there wasn't any significant difference in gene expression. Comparing bone and dentine samples *ctsk* was upregulated by 3.8 folds in the dentine samples and was downregulated by 1.5 folds in the cementum samples when compared with bone samples. In the comparison between cementum and dentin samples *ctsk* was upregulated in dentine samples by 11.3 folds. Apart from known resorption-associated genes, some new possible candidates were identified like *Id1* gene which was upregulated only in cementum samples in comparison with cells differentiated on glass and upregulated by 3.5 folds in cementum samples compared with bone samples. In comparison with dentin this gene was downregulated in dentin samples by 2.7 folds and didn't show any

significant change between bone and dentin samples. The present systematic transcriptome-wide expression study expands our understanding of the interaction between clast cells and mineralized tissues and indicates new possible target genes of relevance for diagnostic and therapeutic strategies.

6. List of figures

- Fig. 1:** longitudinal section of upper central incisor. **13**
- Fig. 2:** Formation of multinucleated osteoclasts from Hematopoietic stem cells the figure shows the critical molecules affecting osteoclasts differentiation like RANKL and M-CSF. Cell-cells fusion forms multinucleated osteoclasts. Mature osteoclast cell is known by the specific genes like Tartrate-resistant acid phosphatase and Cathepsin K. **15**
- Fig. 3:** An osteoclast cell sitting in a Howship's lacuna with the specialized ruffled border that opposes the surface of the bone surface. **16**
- Fig. 4:** Illustration of Mature osteoclasts are attached to bone through $\alpha\beta 3$ -expressing vitronectin receptors and in the sealing zone, osteoclasts form the ruffled border in which proton pump subunits and a chloride channel is present. **17**
- Fig. 5:** A longitudinal section through a cortical bone moving to the left via remodeling process demonstrates the intravascular and perivascular mechanisms for coupling bone resorption (R) to formation (F). Inflammatory cytokines will attract Lymphocytes (L) from the circulation, which in turn will recruit pre-osteoclasts (POcl) with a magnified view illustrates the proposed mechanism for coupling bone resorption to formation via the genetic RANK/RANKL/OPG mechanism. (left) damaged bone stimulates osteocyte to produce inflammatory cytokines. Osteoblasts react by producing RANKL. Differentiated Osteoclasts start resorbing bone which releases growth factors that stimulate the Osteoblasts to release osteoprotegerin (OPG) to stop the differentiation of the osteoclasts. Mononuclear cells build a cementing substance to form a resorption arrest line (shown in green). Preosteoblasts migrate from the circulation and differentiate into Osteoblasts that produce new lamellar bone to fill the resorption cavity. **19**

- Fig. 6:** Illustration of the indirect method of RNA-Sequencing. First, long RNAs are converted into cDNA fragments. Sequencing adaptors (blue) are subsequently added to each cDNA fragment and a short sequence is obtained from each cDNA using high-throughput sequencing technology. The coding sequence obtained from the reads is aligned with the reference transcriptome or so-called Open Reading Frame (ORF) to identify the genes. Reads can be divided into: exonic, junction and poly(A) end-reads. These three types are used to generate a base-resolution expression profile for each gene. **29**
- Fig. 7:** Dentine discs after Gold/palladium sputtering. **32**
- Fig. 8:** Samples loaded in the scanning electron microscope. **33**
- Fig. 9:** Preparation of the extracted teeth to obtain the powder. **34**
- Fig. 10:** Cementum powder after preparation. **34**
- Fig. 11:** Bone powder particles under scanning electron microscope in two different magnifications x25 (big picture) and x250 (small picture to the right). **35**
- Fig. 12:** Dentine powder particles under scanning electron microscope in two different magnifications x25 (big picture) and x250 (small picture to the right). **35**
- Fig. 13:** Cementum powder particles under scanning electron microscope in two different magnifications x25 (big picture) and x250 (small picture to the right). **36**
- Fig. 14:** RAW 264.7 cells under the inverted light microscope (original magnification 10x NA 0.2) after three days of incubation. On the left the sample with 10000 cells and on the right the sample with 50,000 cells can be seen: black areas are the dentine discs the bright areas are RAW264.7 cells. Fusion between the cells is to be identified. attached cells are to be seen on the edge of the discs. **42**

- Fig. 15:** RAW 264.7 cells under the inverted light microscope (original magnification 10x NA 0.2) at the end of incubation. On the left the sample with 10000 cells and on the right the sample with 50,000 cells can be seen: black areas are the dentine discs the bright areas are RAW264.7 cells with some cells in fusion to form osteoclast-like multinucleated cells, attached cells and the irregular edge of the discs are to be seen. **43**
- Fig. 16:** Differentiated RAW264.7 cells on dentine discs under light inverted microscope in two groups: 50000 cells on the left side 10000 cells on the right. Resorption pits on the dentine discs and multinucleated osteoclast-like cell (original magnification 30x NA 0.2). **44**
- Fig. 17:** Dentin discs under scanning electron microscope. High magnification images (A, B Top) show the differentiated osteoclast-like cells with their podosomes (arrows). In low magnification the resorption pits are to be seen (C, D Bottom). **45**
- Fig. 18:** Control sample of RAW 264.7 cells cultured on glass stimulated for 12 days with RANKL and M-CSF then stained with TRAP. A, B show the cells before staining and C, D show the cells after staining with many differentiated TRAP positive osteoclast-like cells (original magnification 10x NA 0.2) **46**
- Fig. 19:** RAW 264.7 cells cultured with bone powder and stimulated for 12 days with RANKL and M-CSF then stained with TRAP. A, B show the cells before staining and C, D show the Cells after staining with many differentiated TRAP positive osteoclast-like cells. (original magnification 10x NA 0.2) **47**
- Fig. 20:** RAW 264.7 cells cultured with dentine powder (red arrows) and stimulated for 12 days with RANKL and M-CSF then stained with TRAP. A, B show the cells before staining and C, D show the cells after staining with many differentiated TRAP positive osteoclast-like cells (black arrows). (original magnification: 10 x NA 0.2) **48**

- Fig. 21:** RAW 264.7 cells cultured with cementum powder (red arrows) and stimulated for 12 days with RANKL and M-CSF then stained with TRAP. A, B show the cells before staining and C, D show the cells after staining with many differentiated TRAP positive osteoclast-like cells (black arrows). (original magnification: 10x NA 0.2) **49**
- Fig. 22:** Bar diagram showing the number of differentially expressed genes between the groups of the samples. (n=4; p <0.05) **50**
- Fig. 23:** Bar diagram shows the number of differentially expressed genes between the groups of the samples after using the logarithm Fold change. (n=4; Log FC ≥ 0.5; p <0.05) **51**
- Fig. 24:** Venn diagram of differentially expressed transcripts (logFC ≥ 0.5; P < 0.05), demonstrating differences and similarities in the number of expressed genes between the negative control group and the other groups of the experiment. **52**
- Fig. 25:** Venn diagram of differentially expressed transcripts (logFC ≥ 0.5; P < 0.05), demonstrating differences and similarities in the number of expressed genes between the positive control group and the other groups of the experiment. **52**
- Fig. 26:** Venn diagram of differentially expressed transcripts (logFC ≥ 0.5; P < 0.05), demonstrating differences and similarities in the number of expressed genes between the three groups of hard tissue samples of the experiment. **53**
- Fig. 27:** Volcano plot showing the change in gene expression level after stimulating RAW264.7 cells with RANKL and M-CSF on glass. Green indicates overexpressed and red indicates repressed genes (logFC ≥ 0.5) Grey indicates genes that didn't show significant change in expression level. The horizontal dashed line represents a significant level of 0.05. **54**

- Fig. 28:** Volcano plot showing the change in gene expression level after stimulating RAW264.7 cells with RANKL and M-CSF on bone tissue. Green indicates overexpressed and red indicates repressed genes ($\log_{2}FC \geq 0.5$) Grey indicates genes that didn't show significant change in expression level. The horizontal dashed line represents a significant level of 0.05. **55**
- Fig. 29:** Volcano plot showing the change in gene expression level after stimulating RAW264.7 cells with RANKL and M-CSF on dentine tissue. Green indicates overexpressed and red indicates repressed genes ($\log_{2}FC \geq 0.5$) Grey indicate genes that didn't show significant change in expression level. The horizontal dashed line represents a significant level of 0.05. **56**
- Fig. 30:** Volcano plot showing the change in gene expression level after stimulating RAW264.7 cells with RANKL and M-CSF on cementum tissue. Green indicates overexpressed and red indicates repressed genes ($\log_{2}FC \geq 0.5$) Grey indicates genes that didn't show significant change in expression level. The horizontal dashed line represents a significant level of 0.05. **57**
- Fig. 31:** Volcano plot showing the change in gene expression level in the RAW264.7 cells stimulated with RANKL and M-CSF on dentine tissue compared to RAW264.7 cells stimulated on cementum tissue. Green indicates overexpressed and red indicates repressed genes ($\log_{2}FC \geq 0.5$) Grey indicates genes that didn't show significant change in expression level. The horizontal dashed line represents a significant level of 0.05. **58**
- Fig. 32:** Volcano plot showing the change in gene expression level in the RAW264.7 cells stimulated with RANKL and M-CSF on cementum tissue compared to RAW264.7 cells stimulated on bone tissue. Green indicates overexpressed and red indicates repressed genes ($\log_{2}FC \geq 0.5$) Grey indicates genes that didn't show significant change in expression level. The horizontal dashed line represents a significant level of 0.05. **59**
- Fig. 33:** Volcano plot showing the change in gene expression level in the RAW264.7 cells stimulated with RANKL and M-CSF on dentine tissue

compared to RAW264.7 cells stimulated on bone tissue. Green indicates overexpressed genes ($\log_{2}FC \geq 0.5$) Grey indicates genes that didn't show significant change in expression level. The horizontal dashed line represents a significant level of 0.05. **60**

Fig. 34: Heat map showing the top 50 regulated transcripts in RAW264.7 cells for the five groups of the sample. The low expression value is colored in blue and the high expression value is in red. Rows represent the genes and are labeled with the gene symbol and columns represent the samples. The sample legend on the right-hand of the heat map indicates which color correspond to which group. The dendrogram on the left-hand side shows clustering of samples as rows and the dendrogram on the top shows clustering of samples as columns. **61**

7. References

Alippe Y, Wang C, Ricci B, Xiao J, Qu C, Zou W, Novack DV, Abu-Amer Y, Civitelli R, Mbalaviele G. Bone matrix components activate the NLRP3 inflammasome and promote osteoclast differentiation. *Scientific reports* 2017; 7: e6630. doi:10.1038/s41598-017-07014-0

Andersen TL, Sondergaard TE, Skorzynska KE. A physical mechanism for coupling bone resorption and formation in adult human bone. *Am J Pathol.* 2009; 174: 239–247

Angel NZ, Walsh N, Forwood MR, Ostrowski MC, Cassady AI, Hume DA. Transgenic Mice Overexpressing Tartrate-Resistant Acid Phosphatase Exhibit an Increased Rate of Bone Turnover. *J Bone Miner Res* 2000; 15: 103 -110

Babaji P, Devanna R, Jagtap K, Chaurasia VR, Jerry JJ, Choudhury BK, Duhan D. The cell biology and role of resorptive cells in diseases: A review. *Annals of African medicine* 2017; 16: 39-45

Benjamini Y, Hochberg Y. Controlling the false discovery rate: a practical and powerful approach to multiple testing. *J R Statist Soc B.*1995; 57: 289–300

Bosshardt DD and Selvig KA. Dental cementum: the dynamic tissue covering of the root. *Periodontology* 2000. 1997; 13: 41-75

Bosshardt DD and Nanci A. Immunolocalization of epithelial and mesenchymal matrix constituents in association with inner enamel epithelial cells. *Journal of Histochemistry & Cytochemistry* 1998; 46: 135–142

Boskey A, Spevak L, Paschalis E. *Calcif Tissue Int* 2002; 71: 145- 152

Battaglino R, Fu J, Spate U, Ersoy U, Joe M, Sedaghat L, Stashenko P. Serotonin regulates osteoclast differentiation through its transporter. *J Bone Miner Res.* 2004; 19: 1420–1431

Boyde A, Ali NN, Jones SJ. Resorption of dentine by isolated osteoclasts in vitro. *British Dental Journal* 1984; 156: 216–220

Brezniak N, Wasserstein A. Orthodontically induced inflammatory root resorption. Part I: The basic science aspects. *Angle Orthodontist* 2002; 72: 175 – 179

Brezniak N, Wasserstein A. Orthodontically induced inflammatory root resorption. Part II: The clinical aspects. *The Angle Orthodontist* 2002; 72: 180–184

Buckwalter JA, Glimcher MJ, Cooper RR, Recker RR. Bone biology. I: Structure, blood supply, cells, matrix, and mineralization. *Instructional course lectures*. 1996; 45: 371-386

Butler WT, Ritchie H. The nature and functional significance of dentin extracellular matrix proteins. *Int J Dev Biol* 1995; 39:169-179

Chan AS, Jensen KK, Skokos D, Doty S, Lederman HK, Kaplan RN, Lyden D. Id1 represses osteoclast-dependent transcription and affects bone formation and hematopoiesis. *PloS one* 2009; 4: e7955. doi: 10.1371/journal.pone.0007955

Chambers TJ, Magnus CJ. Calcitonin alters behaviour of isolated osteoclasts. *J Pathol* 1982; 136: 27–39

Chambers TJ, Revell PA, Fuller K, Athanasou NA. Resorption of bone by isolated rabbit osteoclasts. *J Cell Sci* 1984; 66:383–388

Collin-Osdoby P, Osdoby P. RANKL-mediated osteoclast formation from murine RAW 264.7 cells. *Methods Mol Biol* 2012; 816:187–202

Coxon FP, Rogers MJ, Crockett JC. Isolation and purification of rabbit osteoclasts. *Methods in molecular biology* 2012; 816:145–158

Crick F. Central dogma of molecular biology. *Nature* 1970; 227: 561–563

Cuetara BL, Crotti TN, O'Donoghue AJ and McHugh KP. Cloning and characterization of osteoclast precursors from the RAW264.7 cell line. *In vitro cellular & developmental biology. Animal*. 2006; 42: 182–188

Cui X, Churchill GA. Statistical tests for differential expression in cDNA microarray experiments. *Genome Biol.* 2003; 4: 210-219

Dapunt U, Maurer S, Giese T, Gaida MM, Hänsch GM. The Macrophage Inflammatory Proteins MIP1 (CCL3) and MIP2 (CXCL2) in Implant-Associated Osteomyelitis: Linking Inflammation to Bone Degradation. *Mediators of Inflammation* 2014; Article ID 728619: 10 pages

Darling JM, Goldring SR, Harada Y, Handel ML, Glowacki J, Gravallesse EM. Multinucleated cells in pigmented villonodular synovitis and giant cell tumor of tendon sheath express features of osteoclasts. *Am J Pathol* 1997; 150:1383-1393

Datta HK, Ng WF, Walker JA. The cell biology of bone metabolism. *Journal of Clinical Pathology* 2008; 61: 577-587

Duong L, Rodan G. Regulation of osteoclast formation and function. *Reviews in Endocrine and Metabolic Disorders* 2001; 2: 95–104

Duong LT, Lakkakorpi P, Nakamura I, Rodan GA. Integrins and signaling in osteoclast function. *Matrix Biol.* 2000; 19: 97-105

Detsch R, Mayr H, Ziegler G. Formation of osteoclast-like cells on HA and TCP ceramics. *Acta Biomaterialia* 2008; 4: 139–148

Doi Y, Iwanaga H, Shibutani T, Moriwaki Y, Iwayama Y. Osteoclastic responses to various calcium phosphates in cell cultures. *J Biomed Mater Res* 1999; 47: 424–433

Faccio R, Novack DV, Zallone A, Ross FP, Teitelbaum SL. Dynamic changes in the osteoclast cytoskeleton in response to growth factors and cell attachment are controlled by beta3 integrin. *J Cell Biol* 2003; 4: 499-509

Falkenberg JHF, Harrington MA, Walsh WK. Gene expression and release of macrophage colony stimulating factor in quiescent and proliferating fibroblasts: effects of serum, fibroblast growth promoting factors and IL-1. *Journal of Immunology* 1990; 144: 4657–4662

Fang Z, Cui X. Design and validation issues in RNA-seq experiments. *Briefings in Bioinformatics* 2011; 12: 280–287

Farlex Partner Medical Dictionary, 2012: <https://thefreedictionary.com>. Retrieved May 18 2019

Feyen JHM. Cells of bone; proliferation, differentiation and hormonal regulation. *Physiological Reviews* 1986; 66: 855-886

Fielden MR, Zacharewski TR. Challenges and limitations of gene expression profiling in mechanistic and predictive toxicology. *Toxicological Sciences* 2001; 1: 6–10

Finoulst I, Vink P, Rovers E, Pieterse M, Pinkse M, Bos E, Verhaert P. Identification of low abundant secreted proteins and peptides from primary culture supernatants of human T-cells. *Journal of Proteomics* 2011; 75: 23-33

Fu X, Fu N, Guo S, Yan Z, Xu Y. Estimating accuracy of RNA-Seq and microarrays with proteomics. *BMC genomics* 2009; 10: 161-170

Fuller K, Ross JL, Szewczyk KA, Moss R, Chambers TJ. Bone is not essential for osteoclast activation. *PloS one* 2010; 5: e12837. doi:10.1371/ journal. pone.0012837

Geiger B, Spatz JP, Bershadsky AD. Environmental sensing through focal adhesions. *Nat. Rev. Mol. Cell Biol* 2009;10: 21-33

Goelz L, Buerfent BC, Hofmann A, Ruehl H, Fricker, N, Stamminger W, Oldenburg J, Deschner J, Hoerauf A, Nöthen MM, Schumacher J, Hübner MP, Jaeger AD. Genome-wide transcriptome induced by nickel in human monocytes. *Acta biomaterialia* 2016: 43; 369-382

Goldberg M, Kulkarni AB, Young M, Boskey A. Dentin: structure, composition and mineralization. *Front Biosci (Elite Ed)*. 2011; 3: 711–735

Gonzales C, Hotokezaka H, Yoshimatsu M, Yozgatian JH, Darendeliler MA, Yoshida N. Force magnitude and duration effects on amount of tooth movement and root resorption in the rat molar. *Angle Orthodontist* 2000; 78: 502-509

Götz W, Kunert D, Zhang D. et al. Insulin-like growth factor system components in the periodontium during tooth root resorption and early repair processes in the rat. *European Journal of Oral Sciences* 2006; 114, 318–327

J. Green, S. Schotland, D. J. Stauber, C. R. Kleeman, and T. L. Clemens Cell-matrix interaction in bone: type I collagen modulates signal transduction in osteoblast-like cells *American Journal of Physiology-Cell Physiology* 1995; 268: 1090-1103

Hall TJ, Schaeublin M and Chambers TJ. The majority of osteoclasts require mRNA and protein synthesis for bone resorption in vitro. *Biochem Biophys Res Comm* 1993; 195: 1245-1253

Harokopakis-Hajishengallis E. Physiologic root resorption in primary teeth: Molecular and histological events. *J Oral Sci.* 2007; 49: 1–12

Hart GT, Shaffer DJ, Akilesh S, Brown AC, Moran L, Roopenian DC, Baker P J. Quantitative Gene Expression Profiling Implicates Genes for Susceptibility and Resistance to Alveolar Bone loss. *Infection and Immunity* 2004; 72: 4471-4479. doi: 10.1128/IAI.72.8.4471-4479

Hartsfield J and James K. Personalized orthodontics, the future of genetics in practice. *Seminars in Orthodontics* 2008; 14: 166–171

Hayman AR. Tartrate-resistant acid phosphatase (TRAP) and the osteoclast/immune cell dichotomy. *Autoimmunity* 2008; 41: 218–223

Henriksen K, Karsdal MA, Taylor A, Tosh D, Coxon FP. Generation of human osteoclasts from peripheral blood. *Methods Mol Biol* 2012; 816: 159–175

Henriksen K, Karsdal MA and John Martin T. Osteoclast-derived coupling factors in bone remodeling. *Calcified Tissue International* 2014; 94: 88–97

Helfrich MH, Nesbitt SA, Dorey EL, Horton MA. Rat osteoclasts adhere to a wide range of RGD-Arg-Gly-Asp. peptide-containing proteins, including the bone sialoproteins and fibronectin, via a β_3 integrin. *J. Bone Miner. Res* 1992; 7: 335-343

Holtrop ME, King GJ. The ultrastructure of the osteoclast and its functional implications. *Clin Orthop Relat Res* 1977; 123: 177-96

Hsu H, Lacey DL, Dunstan CR, Solovyev I, Colombero A, Timms E, Tan HL, Elliott G, Kelley MJ, Sarosi I, Wang L, Xia XZ, Elliott R, Chiu L, Black T, Scully S, Capparelli C, Morony S, Shimamoto G, Bass MB, Boyle WJ. Tumor necrosis factor receptor family member RANK mediates osteoclast differentiation and activation induced by osteoprotegerin ligand. *Proc Natl Acad Sci U S A*. 1999; 96: 3540–3545

Humphrey MB and Nakamura MA. A Comprehensive Review of Immunoreceptor Regulation of Osteoclasts. *Clinical Reviews in Allergy & Immunology* 2016; 51: 48-58

Inaoka T, Bilbe G, Ishibashi O, Tezuka K, Kumegawa M, Kokubo T. Molecular cloning of human cDNA for cathepsin K: novel cysteine proteinase predominantly expressed in bone. *Biochem. Biophys. Res. Commun.* 1995; 206: 89–96

Jafari M, Ansari-Pour N. Why, When and How to Adjust Your P Values? *Cell J*. 2019; 20: 604–607

Jeongim Ha, Hyo-Sun Choi, Youngkyun Lee, Hyung-Joo Kwon, Yeong Wook Song, Hong-Hee Kim. CXC Chemokine Ligand 2 Induced by Receptor Activator of NF- κ B Ligand Enhances Osteoclastogenesis. *The Journal of Immunology*, 2010; 184: 4717-4724

Jung Ha Kim, Kabsun Kim, Hye Mi Jin, Bang Ung Youn, Insun Song, Hueng-Sik Choi, Nacksung Kim. Upstream Stimulatory Factors Regulate OSCAR Gene Expression in RANKL-Mediated Osteoclast Differentiation. *Journal of Molecular Biology* 2008; 383: 502-511

Kanehisa J. Time course of escape from calcitonin-induced inhibition of motility and resorption of disaggregated osteoclasts. *Bone* 1989; 10: 125-129

Kim JH, Kim K, Kim I, Seong S and Kim N. NRROS Negatively Regulates Osteoclast Differentiation by Inhibiting RANKL-Mediated NF- κ B and Reactive Oxygen Species Pathways. *Molecules and cells* 2015; 38: 904- 910

Kim K, Kim JH, Lee J, Jin HM, Kook H, Kim KK, Lee SY, Kim N. MafB negatively regulates RANKL-mediated osteoclast differentiation. *Blood* 2007; 109: 3253-3259

Koizumi K, Saitoh Y, Minami T, Takeno N, Tsuneyama K, Miyahara T, Nakayama T, Sakurai H, Takano Y, Nishimura M. Role of CX3CL1/fractalkine in osteoclast differentiation and bone resorption. *Journal of Immunology* 2009;183: 7825–7831

Koskinen C, Persson E, Baldock P, Stenberg Asa, Bostrom I, Matozaki T, Oldenborg P, Lundberg P. Lack of CD47 Impairs Bone Cell Differentiation and Results in an Osteopenic Phenotype in Vivo due to Impaired Signal Regulatory Protein (SIRP) Signaling. *The Journal of biological chemistry* 2013; 8: 288- 295

Kunzler TP, Drobek T, Schuler M, Spencer ND. Systematic study of osteoblast and fibroblast response to roughness by means of surface-morphology gradients. *Biomaterials* 2007; 28: 2175-2182

Lee J, Kim K, Kim JH, Jin HM, Choi HK, Lee S, Kook H, Kim KK, Yokota Y, Lee SY, Choi Y, Kim N. Id helix-loop-helix proteins negatively regulate TRANCE-mediated osteoclast differentiation. *Blood J.* 2006; 107: 2686-2693

Lee NK. Molecular Understanding of Osteoclast Differentiation and Physiology. *Endocrinol Metab.* 2010; 25: 264-269

Li YM, Mitsuhashi T, Wojciechowicz D, Shimizu N, Li J, Stitt A, He C, Banerjee D, Vlassara H. Molecular identity and cellular distribution of advanced glycation endproduct receptors: relationship of p60 to OST-48 and p90 to 80K-H membrane proteins. *Proc Natl Acad Sci U S A.* 1996; 93: 11047–11052

Li YP, Alexander M, Wucherpfennig AL, Yelick P, Chen W, Stashenko P. Cloning and complete coding sequence of a novel human cathepsin expressed in giant cells of osteoclastomas. *Journal of bone and mineral research* 1995; 10: 1197–1202

Liu C, Rangnekar VM, Adamson E, Mercola D. Suppression of growth and transformation and induction of apoptosis by EGR-1. *Cancer Gene Ther.* 1998; 5: 3-28

Lucht U. Osteoclasts, ultrastructure and function. The reticuloendothelial system. A comprehensive treatise. In: Carr I, Deams W, editors. *Morphology.* New York: Plenum Press: 1980: 705-33

Luxenburg C, Geblinger D, Klein E, Anderson K, Hanein D, Geiger B, Addadi L. The architecture of the adhesive apparatus of cultured osteoclasts: from podosome formation to sealing zone assembly. *PLoS One* 2007; 2: e179; <http://dx.doi.org/10.1371/journal.pone.0000179>; PMID: 17264882

Marioni J, Mason C, Mane S, Stephens M, Gilad Y. RNA-Seq: an assessment of technical reproducibility and comparison with gene expression arrays. *Genome Res.* 2008; 18:1509-1514

Martin TJ. and Seeman E. Bone remodelling: its local regulation and the emergence of bone fragility. *Best Practice and Research: Clinical Endocrinology and Metabolism* 2008; 22: 701–722

Martinon F, Burns K, Tschopp J. The inflammasome: a molecular platform triggering activation of inflammatory caspases and processing of proIL-beta. *Mol Cell* 2002; 10: 417–426

Marino S, Logan JG, Mellis D, Capulli M. Generation and cluster of osteoclasts. *Bonekey Rep.* 2014; 570: 1-9

Matsuo K, Galson DL, Zhao C, Peng L, Laplace C, Wang KZ, Bachler MA, Amano H, Aburatani H, Ishikawa H, Wagner EF. Nuclear factor of activated T-cells (NFAT) rescues osteoclastogenesis in precursors lacking c-Fos. *J Biol Chem.* 2004; 279: 26475–26480

Mayer MP, Bukau B. Hsp70 chaperones: cellular functions and molecular mechanism. *Cellular and Molecular Life Sciences* 2005; 62: 670–684

McNab S, Battistutta D, Taverne A, Symons AL. External apical root resorption following orthodontic treatment. *Angle Orthodontist* 2000; 70: 227-232

McSheehy PM and Chambers TJ. Osteoblastic cells mediate osteoclastic responsiveness to parathyroid hormone. *Endocrinology* 1986; 118: 824–828

Mohandesan H, Ravanmehr H, Nasser V. A radiographic analysis of external apical root resorption of maxillary incisors during active orthodontic treatment. *European Journal of Orthodontics* 2007; 29: 134-139

Merrild MH Ditte, Pirapaharan C Dinisha, Andreasen M Christina, Andersen P. Kjærsgaard, Møller MJ Anais, Ding Ming, Delaisse Jean-Marie and Kent Søe. Pit- and trench-forming osteoclasts: a distinction that matters *Bone Research* 2015; 3: e15032; doi:10.1038/boneres.2015.32

Metsis A, Andersson U, Bauren G. Whole-genome expression profiling through fragment display and combinatorial gene identification. *Nucleic Acids Res.* 2004; 32(16): e127. doi: 10.1093/nar/gnh126

Nakamura I, Takahashi N, Sasaki T, Jimi E, Kurokawa T, Suda T. Chemical and physical properties of the extracellular matrix are required for the actin ring formation in osteoclasts. *J. Bone Miner. Res.* 1996; 11: 1873-1879

Nakashima T, Hayashi M, Fukunaga T. Evidence for osteocyte regulation of bone homeostasis through RANKL expression. *Nature Medicine* 2011; 17: 1231–1234

Nakashima T, Hayashi M, Takayanagi H. New insights into osteoclastogenic signaling mechanisms. *Trends in Endocrinology and Metabolism* 2012; 23: 582–590

Naqshbandi A, Sopyan I, Gunawan. Development of Porous Calcium Phosphate Bioceramics for Bone Implant Applications: A Review. *Recent Patents on Materials Science* 2013; 6: 238-252

Narducci P, Nicolin V. Differentiation of activated monocytes into osteoclast-like cells on a hydroxyapatite substrate: an in vitro study. *Ann Anat.* 2009; 191: 349-55

Nesbitt S, Nesbit A, Helfrich M, Horton M. Biochemical characterization of human osteoclast integrins. Osteoclasts express avb3, a2b1, and avb1 integrins. *J. Biol. Chem.* 1993; 268: 16737-16745

Nordstrom T, Shrode LD, Rotstein OD, Romanek R, Goto T, Heersche NM, Manolson MF, Brisseau GF, Grinstein S. Chronic extracellular acidosis induces plasmalemmal vacuolar type H⁺ ATPase activity in osteoclasts. *J Biol Chem.* 1997; 272: 6354-6360

Notsu K, Nakagawa M, Nakamura M. Ubiquitin-like protein MNSF β noncovalently binds to molecular chaperone HSPA8 and regulates osteoclastogenesis. *Molecular and cellular biochemistry.* 2016; 421: 149- 156

Oka H, Miyauchi M, Sakamoto K, Moriwaki S, Niida S, Noguchi K. PGE2 activates cementoclastogenesis by cementoblasts via EP4. *J Dent Res.* 2007; 86: 974–979

Olivieri JG, Duran SF, Mercade M, Pe´rez N, Roig M. Treatment of a perforating inflammatory external root resorption with mineral trioxide aggregate and histologic examination after extraction. *J Endod.* 2012; 38: 1007-1011

Oliveros JC. Venny. An interactive tool for comparing lists with Venn's diagrams 2007. <http://bioinfogp.cnb.csic.es/tools/venny/index.html>

Oshiro T, Shibasaki Y, Martin TJ, Sasaki T. Immunolocalization of vacuolar-type H-ATPase, cathepsin K, matrix metalloproteinase-9, and receptor activator of NFkappa B ligand in odontoclasts during physiological root resorption of human deciduous teeth. *Anat Rec.* 2001; 264: 305- 311

Oshiro T, Shiotani A, Shibasaki Y, Sasaki T. Osteoclast induction in periodontal tissue during experimental movement of incisors in osteoprotegerin-deficient mice. *Anat Rec.* 2002; 266: 218- 225

Owens J and Chambers TJ. Macrophage colony-stimulating factor (M-CSF) induces migration in osteoclasts in vitro. *Biochem Biophys Res Comm.* 1993; 195: 1401- 1407

Papatheodorou I, Oellrich A, Smedley D. Linking gene expression to phenotypes via pathway information. *J Biomed Semantics* 2015; 6: 10-17

Peterlin BM, Brogie JE, Price DH. 7SK snRNA: a noncoding RNA that plays a major role in regulating eukaryotic transcription. *Wiley Interdisciplinary Reviews: RNA* 2012; 3: 92–103

Pita-Jua´rez Y, Altschuler G, Kariotis S, Wei W, Koler K, Green C, et al. The Pathway Coexpression Network: Revealing pathway relationships. *PLoS Comput Biol* 2018; 14: e1006042. <https://doi.org/10.1371/journal.pcbi.1006042>

Purdue PE, Crotti TN, Shen ZX, Swantek J, Li J, Hill J. Comprehensive profiling analysis of actively resorbing osteoclasts identifies critical signaling pathways regulated by bone substrate. *Sci Rep.* 2014; 4: 7595

Puissant E and Boonen M. Monocytes/Macrophages Upregulate the Hyaluronidase HYAL1 and Adapt Its Subcellular Trafficking to Promote Extracellular Residency upon Differentiation into osteoclasts. *PloS one* 2016; 11: e0165004. doi: 10.1371/journal.pone.0165004

Quinn JM, Elliott J, Gillespie MT, Martin TJ. A combination of osteoclast differentiation factor and macrophage-colony stimulating factor is sufficient for both human and mouse osteoclast formation in vitro. *Endocrinology.* 1998a; 139: 4424–4427

Raggatt LJ, Partridge NC. Cellular and molecular mechanisms of bone remodeling. *J Biol Chem.* 2010; 285: 25103–25108

Richard D, Emes, LG, Eitan E, Winter, CP. Comparison of the genomes of human and mouse lays the foundation of genome zoology, *Human Molecular Genetics*; 2003; 12: 701–709

Ritchie ME, Phipson B, Wu D. Limma powers differential expression analyses for RNA-Sequencing and microarray studies. *Nucleic Acids Res* 2015;43: e47

Roberto FM, Beltrao RTS, Janson G, Henriques JFC, Chiqueto K. Evaluation of root resorption after open bite treatment with and without extractions. *American Journal of Orthodontics and Dentofacial Orthopedics* 2007; 143: 15-22

Roberts WE, Huja S, Roberts JA. Bone modeling: biomechanics, molecular mechanisms, and clinical perspectives. *Sem Orthod* 2004; 10: 123-161

Roberts WE, Wood HB, Chambers DW, Burk DT. Vascularly oriented differentiation gradient of osteoblast precursor cells in rat periodontal ligament: implications for osteoblast histogenesis and periodontal bone loss. *Journal of Periodontal Research* 1987b; 22: 461– 467

Roberts WE, Roberts JA, Epker BN. Remodeling of mineralized tissues, Part I: The Frost legacy. *Seminars in Orthodontics* 2006b; 12: 216–237

Roberts WE and Hartsfield JK. Bone development and function: Genetic and environmental mechanisms. *Seminars in Orthodontics* 2004; 10: 100–122

Roodman GD. Regulation of osteoclast differentiation. *Ann N Y Acad Sci* 2006;1068: 100-109

Rumpler M, Würger T, Roschger P, Zwettler E, Peterlik H, Fratzl P, Klaushofer K. Microcracks and osteoclast resorption activity in vitro. *Calcified tissue international* 2012; 90: 230- 238

Rumpler M, Würger T, Roschger P, Zwettler E, Sturmlechner I, Altmann P, Fratzl P, Rogers MJ, Klaushofer K. Osteoclasts on bone and dentin in vitro: mechanism of trail formation and comparison of resorption behavior. *Calcified tissue international* 2013; 93: 526-539

Saltel F, Destaing O, Bard F, Eichert D, Jurdic P. Apatite-mediated actindynamics in resorbing osteoclasts. *Mol. Biol. Cell* 2004; 15: 5231–5241

Sanuki R, Shionome C, Kuwabara A. Compressive force induces osteoclast differentiation via prostaglandin E (2) production in MC3T3-E1 cells. *Connective Tissue Research* 2010; 51: 150–158

Satoh T, Kidoya H, Naito H, Yamamoto M, Takemura N, Nakagawa K, Yoshioka Y, Morii E, Takakura N, Takeuchi O, Akira S. Critical role of Trib1 in differentiation of tissue-resident M2-like macrophages. *Nature* 2013; 495: 524-528

Schilke R, Lisson JA, Bauß O, Geurtsen W. Comparison of the number and diameter of dentinal tubules in human and bovine dentine by scanning electron microscopic investigation. *Archives of Oral Biology* 2000; 45: 355-361

Shafer WG, Hine MK, Levy BM. *A Textbook of Oral Pathology*, 2nd Edition, W. B. Saunders Company, Philadelphia, 1963: 217

Sriarj W, Aoki K, Ohya K, Takagi Y, Shimokawa H. Bovine dentine organic matrix down-regulates osteoclast activity. *J Bone Miner Metab.* 2009; 27: 315–323

Suda T, Takahashi N, Martin TJ. Modulation of osteoclast differentiation. *Endocr. Rev.* 1992; 13: 66–80

Stahlberg A, Kubista M, Aman P. Single-cell gene-expression profiling and its potential diagnostic applications. *Expert Rev Mol Diagn.* 2011; 11: 735–740

Steiniger B, Schwarzbach H, Stachniss V. *Mikroskopische Anatomie der Zähne und des Parodonts* 1. Auflage. Stuttgart: Thieme; 2010

Stern R. Devising a pathway for hyaluronan catabolism: are we there yet? *Glycobiology* 2003; 13: 105–115

Taciak B, Bialasek M, Braniewska A, Sas Z, Sawicka P, Kiraga L, Rygiel T, Krol M. Evaluation of phenotypic and functional stability of RAW 264.7 cell line through serial passages. *PLoS ONE* 2018; 13: art. no. e0198943

Takahashi N, Yamana H, Yoshiki S, Roodman GD, Mundy GR, Jones SJ, Boyde A, Suda T. Osteoclast-like cell formation and its regulation by osteotropic hormones in mouse bone marrow cultures. *Endocrinology* 1988; 122: 1373–1382

Takahashi N, Udagawa N, Suda T. A new member of tumor necrosis factor ligand family, ODF/OPGL/TRANE/RANKL, regulates osteoclast differentiation and function. *Biochem Biophys Res Commun* 1999; 256: 449–455

Teitelbaum SL. Bone resorption by osteoclasts. *Science* 2000; 289: 1504-1508

Thomas GP, Baker SU, Eisman JA, Gardiner EM. Changing RANKL/OPG mRNA expression in differentiating murine primary osteoblasts. *J Endocrinol* 2001; 170: 451-460

Tyrovola JB, Spyropoulos MN, Makou M, Perrea D. Root resorption and the OPG/RANKL/RANK system: A mini review. *J Oral Sci.* 2008; 50: 367–376

Vesprey A. and Yang W. Pit Assay to Measure the Bone Resorptive Activity of Bone Marrow-derived osteoclasts. *Bio-protocol* 2016; 6: e1836

Wang Y, Nishida S, Elalieh HZ., Long RK., Halloran BP, Bikle DD. Role of IGF-I Signaling in Regulating osteoclastogenesis. *J Bone Miner Res.* 2006; 21: 1350-1358

Wang Z, Gerstein M, Snyder M. RNA-Seq: a revolutionary tool for transcriptomics. *Nat Rev Genet.* 2009; 10: 57-63

Wang Z and McCauley LK. osteoclasts and odontoclasts: Signaling pathways to development and disease. *Oral Dis.* 2011; 17: 129–142

Waterston RH, Lindblad TK, Birney E, Rogers J, Abril JF, Agarwal P, Agarwala R, Ainscough R, Alexandersson M, An P. Initial sequencing and comparative analysis of the mouse genome. *Nature* 2002; 420: 520–562

Westhrin M, Moen SH, Holien T, Mylin AK, Heickendorff L, Olsen OE, Sundan A, Turesson I, Gimsing P, Waage A, Standal T. Growth differentiation factor 15 (GDF15) promotes osteoclast differentiation and inhibits osteoblast differentiation and high serum GDF15 levels are associated with multiple myeloma bone disease. *Haematologica* 2015;100: e511-4

Weivoda MM, Ruan M, Hachfeld CM, Pederson L, Howe A, Davey RA, Zajac, JD, Kobayashi Y, Williams BO, Westendorf JJ, Khosla S, Oursler MJ. Wnt Signaling Inhibits osteoclast Differentiation by Activating Canonical and Noncanonical cAMP/PKA Pathways. *Journal of bone and mineral research* 2015; 31: 65-75

Willingham SB, Volkmer J, Gentles AJ, Sahoo D, Dalerba P, Mitra SS, Wang J, Contreras TH, Martin R, Cohen JD, Lovelace PA, Scheeren FA, Chao MP, Weiskopf

K, Tang C, Volkmer AK, Naik TJ, Storm TA, Mosley AR, Edris B, Schmid SM, Sun CK, Chua M, Murillo O, Rajendran PS, Cha AC, Chin RK, Kim D, Adorno M, Raveh T, Tseng D, Jaiswal S, Enger P, Steinberg GK, Li G, So SK, Majeti R, Harsh GR, Rijn MV, Teng NN, Sunwoo JB, Alizadeh AA, Clarke MF, Weissman IL. The CD47-signal regulatory protein alpha (SIRPa) interaction is a therapeutic target for human solid tumors. *Proceedings of the National Academy of Sciences of the United States of America* 2012; 109: 6662-6667

Xiong J, Onal M, Jilka RL. Matrix-embedded cells control osteoclast formation. *Nature Medicine* 2011; 17: 1235–1241

Yamamoto T, Hasegawa T, Hongo H, Amizuka N. Histology of human cementum: Its structure, function, and development. *Japanese Dental Science Review* 2016; 52: 10-16

Yasuda H, Shima N, Nakagawa N, Yamaguchi K, Kinosaki M, Mochizuki S, Tomoyasu A, Yano K, Goto M, Murakami A, Tsuda E, Morinaga T, Higashio K, Udagawa N, Takahashi N, Suda T. osteoclast differentiation factor is a ligand for osteoprotegerin/ osteoclastogenesis inhibitory factor and is identical to TRANCE/RANKL. *Proc. Natl. Acad. Sci.*1998; 95: 3597–3602

Zambonin ZA, Teti A, Pace G, Covelli V. Quantitative evaluation of experimentally induced osteocytic osteoplasia in hen's femur. *Boll Soc Ital Biol Sper* 1980; 56:1038–1044

Zhao S, Fung-Leung W-P, Bittner A, Ngo K, Liu X. Comparison of RNA-Seq and Microarray in Transcriptome Profiling of Activated T Cells. *PLoS ONE* 2014; 9: e78644. doi: 10.1371/journal.pone.0078644

8. Acknowledgment

Professor Dr.med.dent. A.Jäger, Chair of the department of orthodontics, center of Dento-Maxillo-Facial medicine, faculty of medicine, University of Bonn. I would like to express my gratitude for serving as my thesis director and mentor through the research process, for the permission to use the laboratories and for the correction suggestions in my thesis.

Professor Dr.med.dent L. Gölz, Chair of the department of orthodontics, center of Dento-Maxillo-Facial medicine, faculty of medicine, University of Erlangen. I should express my appreciation for her guidance, declarations and support during the preparation of this thesis.

Professor Dr.med.dent. M. Wolf, M.Sc., Chair of the department of orthodontics, center of Dento-Maxillo-Facial medicine, faculty of medicine, University of Aachen. I acknowledge his contribution in the selection of this research topic.

Dr.rer.nat. André Heimbach, Head of NGS Core Facility of the medical faculty, institute of human genetics, department of genomics, life & brain center, university of Bonn. I should thank the scientific and technical support in this research.

Mrs. J. Marciniak, biological technical assistant at the department of orthodontics, center of Dento-Maxillo-Facial medicine, faculty of medicine, University of Bonn. I am thankful for the technical assistance through the experimental work for this thesis.